YAEC-1935

Vermont Yankee
Cycle 19
Core Performance Analysis Report

October 1996

Major Contributors:

C. Chiu
N. Fujita
B. Hubbard
D. Kapitz
M. LeFrancois
D. Morin
K. Morrissey
J. Neyman
L. Schor
F. Seifaee
R. Smith
K. StJohn
R. Weader
R. Woehlke

Prepared by: M A Stronen 10/11/96

M. A. Stronen (Date)
VY Nuclear Engineering Coordinator

Approved by: R J Cacciapouti 10/11/96

R. J. Cacciapouti, Manager (Date)
Reactor Physics Group

Approved by: P. A. Bergeron 10/11/96

P. A. Bergeron, Manager (Date)
Transient Analysis Group

Approved by: R Sundaram 10/11/96

R. K. Sundaram, Manager (Date)
LOCA Analysis Group

Approved by: R J Cacciapouti Jr 10/11/96

J. R. Chapman, Director (Date)
Nuclear Engineering Department

Approved by: M. J. Marian 10/11/96

M. J. Marian (Date)
Nuclear Services Manager

Yankee Atomic Electric Company
Nuclear Services Division
580 Main Street
Bolton, Massachusetts 01740

DISCLAIMER OF RESPONSIBILITY

This document was prepared by Yankee Atomic Electric Company ("Yankee"). The use of information contained in this document by anyone other than Yankee, or the Organization for which this document was prepared under contract, is not authorized and, with respect to any unauthorized use, neither Yankee nor its officers, directors, agents, or employees assume any obligation, responsibility, or liability or make any warranty or representation as to the accuracy or completeness of the material contained in this document.

ABSTRACT

This report presents design information, calculational results, and operating limits pertinent to the operation of Cycle 19 of the Vermont Yankee Nuclear Power Station. These include the fuel design and core loading pattern descriptions; calculated reactor power distributions, exposure distributions, shutdown capability, and reactivity data; and the results of the transient, accident and stability analyses performed to justify plant operation throughout the cycle.

ACKNOWLEDGMENTS

The author and major contributors would like to acknowledge the contributions to this work by the Vermont Yankee Reactor Engineering Department for their review of input data and guidance.

TABLE OF CONTENTS

TABLE OF CONTENTS

(Continued)

TABLE OF CONTENTS
(Continued)

LIST OF TABLES

LIST OF TABLES
(Continued)

LIST OF FIGURES

LIST OF FIGURES
(Continued)

1.0 INTRODUCTION

This report provides information to support the operation of the Vermont Yankee Nuclear Power Station through the forthcoming Cycle 19. In this report, Cycle 19 will be referred to as the Reload Cycle. The preceding Cycle 18 will be referred to as the Current Cycle. The Cycle 18/19 refueling will involve the discharge of 120 irradiated fuel bundles and the insertion of 120 new fuel bundles. The resultant core will consist of 120 new fuel bundles and 248 irradiated fuel bundles. The General Electric Company (GE) manufactured all the bundles. Some of the irradiated fuel was also present in the reactor in Cycle 17. This cycle will be referred to as the Past Cycle.

This report contains descriptions and analyses results pertaining to the mechanical, thermal-hydraulic, physics, transient analyses, accident analyses and stability analysis of the Reload Cycle. The MAPLHGR and MCPR operating limits and the stability exclusion and buffer regions calculated for the Reload Cycle are given in Appendix A. These limits will be included in the Core Operating Limits Report.

2.0 RECENT REACTOR OPERATING HISTORY

2.1 Operating History of the Current Cycle

The current operating cycle is Cycle 18. The Current Cycle operated at, or near, full power with the exception of sequence exchanges, several power reductions, one short repair outage and a coastdown to the end of cycle. The operating history highlights and control rod sequence exchange schedule of the Current Cycle are found in Table 2.1.1.

2.2 Operating History of Past Applicable Cycle

The irradiated fuel in the Reload Cycle includes some fuel bundles initially inserted in Cycle 17. This Past Cycle operated at, or near, full power with the exception of sequence exchanges, several short power reductions, four short repair outages and a coastdown to the end of cycle. The operating history highlights of the Past Cycle are found in Table 2.2.1. The Past Cycle is described in detail in the Cycle 17 Summary Report[1].

TABLE 2.1.1

VY CYCLE 18 OPERATING HIGHLIGHTS

Beginning of Cycle Date	May 2, 1995
End of Cycle Date	September 7, 1996*
Weight of Uranium As-Loaded (Short Tons)	72.12
Beginning of Cycle Core Average Exposure** (MWd/St)	12316**
End of Full Power Core Average Exposure** (MWd/St)	21930*
End of Cycle Core Average Exposure** (MWd/St)	22650*
Number of Fresh Assemblies	120
Number of Irradiated Assemblies	248

Control Rod Sequence Exchange Schedule:

	Sequence	
Date	From	To
July 11, 1995	A2-1	B2-1
September 11, 1995	B2-1	A1-1
November 7, 1995	A1-1	B1-1
January 9, 1996	B1-1	A2-2
February 27, 1996	A2-2	B2-2
April 23, 1996	B2-2	A1-2
June 12, 1996	A1-2	B1-2

---

* Projected dates and exposures assumed for licensing. The actual End of Cycle Core Average Exposure was 22,964 MWd/St.

** Exposures based on the Plant Process Computer accounting.

TABLE 2.2.1

VY CYCLE 17 OPERATING HIGHLIGHTS

Beginning of Cycle Date	October 24, 1993
End of Cycle Date	March 17, 1995
Weight of Uranium As-Loaded (Short Tons)	72.02
Beginning of Cycle Core Average Exposure* (MWd/St)	11547
End of Full Power Core Average Exposure* (MWd/St)	21603
End of Cycle Core Average Exposure* (MWd/St)	22156
Number of Fresh Assemblies	128
Number of Irradiated Assemblies	240

Control Rod Sequence Exchange Schedule:

	Sequence	
Date	From	To
January 9, 1994	A2-1	B2-1
March 15, 1994	B2-1	A1-1
May 17, 1994	A1-1	B1-1
July 19, 1994	B1-1	A2-2
October 6, 1994	A2-2	B2-2
December 2, 1994	B2-2	A1-2
January 24, 1995	A1-2	B1-2

* Exposures based on the Plant Process Computer accounting.

3.0 RELOAD CORE DESIGN DESCRIPTION

3.1 Core Fuel Loading

The Reload Cycle core will consist of both new and irradiated assemblies. All the assemblies have bypass flow holes drilled in the lower tie plate. Table 3.1.1 characterizes the core by fuel type, batch size, and first cycle loaded. A description of the fuel is found in the GE Standard Application for Reactor Fuel[2] and the GE Fuel Bundle Design Reports[3],[4].

3.2 Design Reference Core Loading Pattern

The Reload Cycle assembly locations are indicated on the map in Figure 3.2.1. The other quadrants are mirror images with bundles of the same type having nearly identical exposures. The bundles are identified by the reload number in which they were first introduced into the core. Table 3.1.1 provides the key, called bundle ID, which identifies what explicit fuel type is found in each bundle location.

If any changes are made to the loading pattern at the time of refueling, they will be evaluated under 10CFR50.59. The final loading pattern with specific fuel bundle serial numbers will be supplied in the Startup Test Report.

3.3 Assembly Exposure Distribution

The assumed nominal exposure on the fuel bundles in the Reload Cycle design reference loading pattern is given in Figure 3.2.1. To obtain this exposure distribution, the Past Cycle was depleted with the SIMULATE-3 model[5],[6] using actual plant operating history. For the Current Cycle, plant operating history was used through September 18, 1995. Beyond this date, the exposure was accumulated using a best-estimate rodded depletion analysis to End of Cycle (EOC).

Table 3.3.1 gives the assumed nominal exposure on the Current Cycle and the Beginning of Cycle (BOC) core average exposure that results from the shuffle into the Reload Cycle loading pattern. The Reload Cycle End of Full Power Life (EOFPL) core average exposure and cycle capability are provided.

TABLE 3.1.1

ASSUMED VY CYCLE 19 FUEL BUNDLE TYPES AND NUMBERS

	Fuel Type Designation	Reload Bundle ID	Cycle Loaded	Number of Bundles
Irradiated	BP8DWB335-10GZ	R16A	17	96
	BP8DWB335-11GZ	R16B	17	32
	BP8DWB335-10GZ	R17A	18	88
	BP8DWB335-11GZ	R17B	18	32
New	BP8DWB354-12GZ	R18	19	120

TABLE 3.3.1

DESIGN BASIS VY CYCLE 18 AND CYCLE 19 EXPOSURES*

Assumed End of Current Cycle Core Average Exposure with an Exposure Window of + 600 MWd/St[7]	22.46+0.6 GWd/St
Assumed Beginning of Reload Cycle Core Average Exposure	12.23 GWd/St
Haling Calculated End of Full Power Life Reload Cycle Core Average Exposure	22.93 GWd/St
Reload Cycle Full Power Exposure Capability (Haling)	10.70 GWd/St

* Exposures based on the SIMULATE-3 accounting.

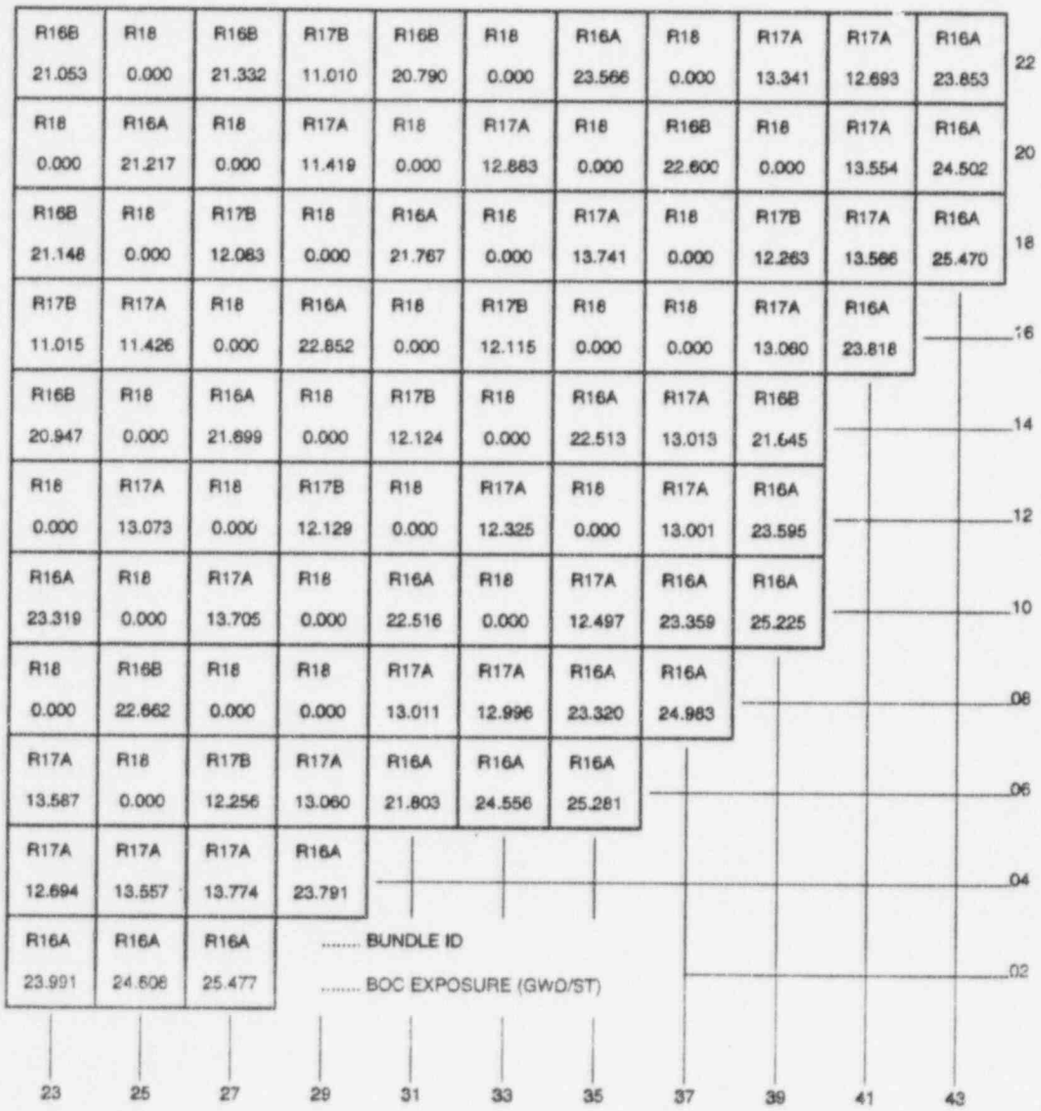

FIGURE 3.2.1

VY CYCLE 19 DESIGN REFERENCE LOADING PATTERN, LOWER RIGHT QUADRANT

4.0 FUEL MECHANICAL AND THERMAL DESIGN

4.1 Mechanical Design

All of the fuel to be inserted into the Reload Cycle was fabricated by GE. The major mechanical design parameters are given in Table 4.1.1 and References 2 through 4. Detailed descriptions of the fuel rod mechanical design and mechanical design analyses are provided in Reference 2. These design analyses remain valid with respect to the Reload Cycle operation. Mechanical and chemical compatibility of the fuel bundles with the in-service reactor environment is also addressed in Reference 2.

4.2 Thermal Design

The fuel thermal effects calculations were performed using the FROSSTEY-2 computer code[8]. The FROSSTEY-2 code calculates pellet-to-cladding gap conductance and fuel temperatures from a combination of theoretical and empirical models including but not limited to fuel and cladding thermal expansion, fission gas release, pellet swelling, pellet densification, pellet cracking, and fuel and cladding thermal conductivity.

The thermal effects analysis included the calculation of fuel temperatures and pellet-to-cladding gap conductance under core average and hot channel conditions. The core average calculations integrate the responses of individual fuel batch average operating histories over the core average exposure range of the Reload Cycle. These gap conductance values are weighted axially into 12 axial nodes by power distributions and radially by volume. The core-wide gap conductance values for the RETRAN system simulations, described in Sections 7.1 and 7.2, are from this data set at the corresponding exposure statepoints. Table 4.2.1 provides the core average response of gap conductance.

The hot channel gap conductance values, which are input to the hot channel transient calculations (Section 7.1), were evaluated for the limiting fuel bundle type as a function of the assembly exposure for two axial power shapes, a 1.4 chopped cosine and the Reload Cycle's Haling. The hot channel calculations assumed the following as required by the NRC Safety Evaluation for

FROSSTEY-2[9]: 1) appropriate allowances to account for manufacturing uncertainties and 2) the worst axial power shape prior to the transient. The peak power node was placed at the maximum average planar linear heat generation rate (MAPLHGR) limits. Gap conductance values for the hot channel analysis were determined using the limiting bundle exposure. The limiting bundle is defined as the bundle with the lowest MCPR or the highest power, if different, within the exposure range of interest. The limiting exposure for the bundle is defined by the exposure which produces the highest bundle average gap conductance within the interval of interest. The SIMULATE-3 rodded depletion (Section 5.1.2) provided predictions of the limiting bundle exposure for each exposure interval. Table 4.2.2 provides the hot channel gap conductance values for the two axial power shapes. Results are presented for the bounding exposure for the chopped cosine shape and at the four exposure statepoints for the Haling shape.

4.3 Operating Experience

All irradiated fuel bundles scheduled to be reinserted in the Reload Cycle have operated as expected in past cycles of Vermont Yankee. Off-gas measurements in the Current Cycle indicate no fuel rod failure.

TABLE 4.1.1

NOMINAL FUEL MECHANICAL DESIGN PARAMETERS

Fuel Bundle*	Irradiated Fuel Type	New Fuel Types
Bundle Types	GE8X8NB	GE8X8NB
Vendor Designation	GE9B-P8DWB335-10GZ & GE9B-P8DWB335-11GZ	GE9B-P8DWB354-12GZ
Initial Enrichment, w/o U_{235}	3.35	3.54
Rod Array	8X8	8X8
Fuel Rods per Bundle	60	60
Outer Fuel Channel		
Material	Zr-2	Zr-2
Wall Thickness, inches	0.080	0.080

* Complete bundle, rod, and pellet descriptions are found in References 2 through 4.

TABLE 4.2.1

VY CYCLE 19 CORE AVERAGE GAP CONDUCTANCE VALUES

Axial Node	Gap Conductance (BTU/hr-ft^2-°F) BOC	EOFPL-2000 MWd/St	EOFPL-1000 MWd/St	EOFPL
1	1125	1890	2035	2095
2	2405	3630	3710	3885
3	2555	3840	3955	4435
4	2580	3860	4015	4610
5	2610	3900	4075	4665
6	2645	3930	4160	4670
7	2605	3895	4075	4620
8	2610	3890	4080	4675
9	2535	3825	3930	4345
10	2450	3710	3805	4035
11	1940	3025	3080	3235
12	685	1085	1145	1245

TABLE 4.2.2

VY CYCLE 19 HOT CHANNEL GAP CONDUCTANCE VALUES*

FOR HALING AXIAL POWER DISTRIBUTION

Axial Node	Gap Conductance (BTU/hr-ft^2-°F)			
	BOC**	EOFPL-2000 MWd/St**	EOFPL-1000 MWd/St**	EOFPL**
	7.63 GWd/St***	11.02 GWd/St***	11.02 GWd/St***	12.17 GWd/St***
1	3970	5280	5280	5080
2	8110	7780	7780	8110
3	9250	10200	10200	9830
4	9280	10200	10200	9830
5	9340	10200	10200	9830
6	9460	10200	10200	9820
7	9350	10200	10200	9820
8	9330	10200	10200	9820
9	9210	10200	10200	9820
10	8470	8160	8160	9030
11	7250	7140	7140	7120
12	2050	2630	2630	3080

---

* The hot channel gap conductance values are derived for the BP8DWB354 fuel type because it is conservative compared to the other fuel types.

** Core Average Exposure.

*** Peak Bundle Exposure.

TABLE 4.2.3

VY CYCLE 19 HOT CHANNEL GAP CONDUCTANCE VALUES*

FOR 1.4 CHOPPED COSINE AXIAL POWER DISTRIBUTION

Axial Node	Gap Conductance (BTU/hr-ft^2-°F)			
	BOC**	EOFPL-2000 MWd/St**	EOFPL-1000 MWd/St**	EOFPL**
	7.15 GWd/St***	11.03 GWd/St***	11.43 GWd/St***	12.80 GWd/St***
1	1050	1000	1000	990
2	1790	2420	2510	2790
3	4390	6560	6700	6420
4	7880	8070	8000	7740
5	8920	9810	10340	9840
6	9850	10500	10350	9850
7	9490	10500	10350	9850
8	9760	10500	10350	9850
9	8150	10500	8460	9440
10	6640	7320	7420	7380
11	2820	4770	5060	5090
12	1230	1280	1290	1330

---

* The hot channel gap conductance values are derived for the BP8DWB354 fuel type because it is conservative compared to the other fuel types.

** Core Average Exposure.

*** Peak Bundle Exposure.

5.0 NUCLEAR DESIGN

5.1 Core Power Distributions

The Reload Cycle was depleted using SIMULATE-3 to give both a rodded depletion and an All Rods Out (ARO) Haling depletion.

5.1.1 Haling Power Distribution

The Haling depletion serves as the basis for defining core reactivity characteristics for most transient evaluations. This is primarily because its flat power shape has conservatively weak scram characteristics. Sensitivity studies have shown that the limiting pressurization transient results are more conservative when calculated using the Haling power distribution as the initial power shape.

The Haling power distribution is calculated in the ARO condition. The Haling iteration converges on a self-consistent power and exposure distribution for the burnup step to EOFPL. In principle, this should provide the overall minimum peaking power shape for the cycle. During the actual cycle, flatter power distributions might occasionally be achieved by shaping with control rods. However, such shaping would leave under burned regions in the core which would peak at another point in time. Figures 5.1.1 and 5.1.2 give the Haling radial and axial average power distributions for the Reload Cycle.

5.1.2 Rodded Depletion Power Distribution

The rodded depletion was used to evaluate the misloaded bundle error and the rod withdrawal error because it provides the initial rod patterns and more accurately defines the local characteristics prior to the transient evaluations. It was also used in the rod drop worth and shutdown margin calculations because it depletes the top of the core more realistically than the Haling depletion. The rodded depletion also provides the hot channel bundle exposures for the gap conductance calculation.

To generate the rodded depletion, control rod patterns were developed which give critical eigenvalues at several points in the cycle and peaking similar to the Haling calculation. The resulting patterns were frequently more peaked than the Haling, but were below expected operating limits.

However, as stated above, the under burned regions of the core can exhibit peaking in excess of the Haling peaking when pulling ARO at EOFPL. Figures 5.1.3 and 5.1.4 give the ARO radial and axial average power distributions for the Reload Cycle rodded depletion at EOFPL.

5.2 Core Exposure Distributions

The Reload Cycle exposures are summarized in Table 3.3.1. The projected BOC radial exposure distribution for the Reload Cycle is given in Figure 3.2.1. The Haling calculation produced the EOFPL radial exposure distribution given in Figure 5.2.1. Since the Haling power shape is constant, it can be held fixed by SIMULATE-3 to give the exposure distributions at various mid-cycle points; that is: EOFPL-2000 MWd/St and EOFPL-1000 MWd/St. These exposure distributions together with the BOC and EOFPL distributions were used to develop reactivity input for the core wide transient analyses.

The rodded depletion differs from the Haling during the cycle because the rods shape the power differently. However, rod sequences are swapped frequently and the overall exposure distribution at end of cycle is similar to the Haling. Figure 5.2.2 gives the EOFPL radial exposure distribution for the Reload Cycle rodded depletion.

5.3 Cold Shutdown Margin

The shutdown margin (SDM) for the Reload Cycle must exceed the Technical Specifications SDM limit [10]. Using SIMULATE-3, a search was made for the strongest worth control rod at various exposures in the cycle. This is necessary because rod worths change with exposure on adjacent assemblies. Then the cold K_{eff} with the strongest rod out was calculated at BOC and at various exposure points during the cycle. Subtracting each cold K_{eff} with the strongest rod out from the cold critical K_{eff} defines the SDM as a function of exposure. Figure 5.3.1 shows the results.

The cold critical K_{eff} was defined as the average calculated critical K_{eff} minus a 95% confidence level uncertainty. Then all cold results were normalized to make the critical K_{eff} equal to 1.000.

Because the local reactivity may increase with exposure, the SDM may decrease. To account for this and other uncertainties, the value R is calculated. R is defined as R_1 plus R_2. R_1 is the difference

between the cold K_{eff} with the strongest rod out at BOC and the maximum cold K_{eff} with the strongest rod out in the cycle. R_2 is a measurement uncertainty in the demonstration of SDM associated with the manufacture of past control blades. It is presently set at 0.07% ΔK[11],[12]. The shutdown margin results, summarized in Table 5.3.1, are greater than the Technical Specification limit including R.

5.4 Maximum K_∞ for the Spent Fuel Pool

Section 5.5E of the Technical Specifications requires that the K_∞ for any bundle stored in either the new fuel vault or the spent fuel pool not exceed 1.31 to ensure compliance with the K_{eff} safety limit of 0.95. The bundles used in the Reload Cycle do not exceed the specifications in Section 5.5E, as shown in Table 5.4.1. These values are obtained from CASMO-3G[13].

TABLE 5.3.1

VY CYCLE 19 K_{EFF} VALUES AND SHUTDOWN MARGIN CALCULATION

Cold Critical K_{eff}	1.0000
BOC K_{eff} - Controlled With Strongest Worth Rod Withdrawn	0.9883
Cycle Minimum Shutdown Margin Occurs at 8400 MWd/St With Strongest Worth Rod Withdrawn	1.15% ΔK
R_1, Maximum Increase in Cold K_{eff} With Exposure	0.018% ΔK

TABLE 5.4.1

VY CYCLE 19 MAXIMUM COLD K_∞ OF ANY ENRICHED SEGMENT

Bundle Type	Maximum K_∞
BP8DWB335-10GZ	1.22
BP8DWB335-11GZ	1.22
BP8DWB354-12GZ	1.22

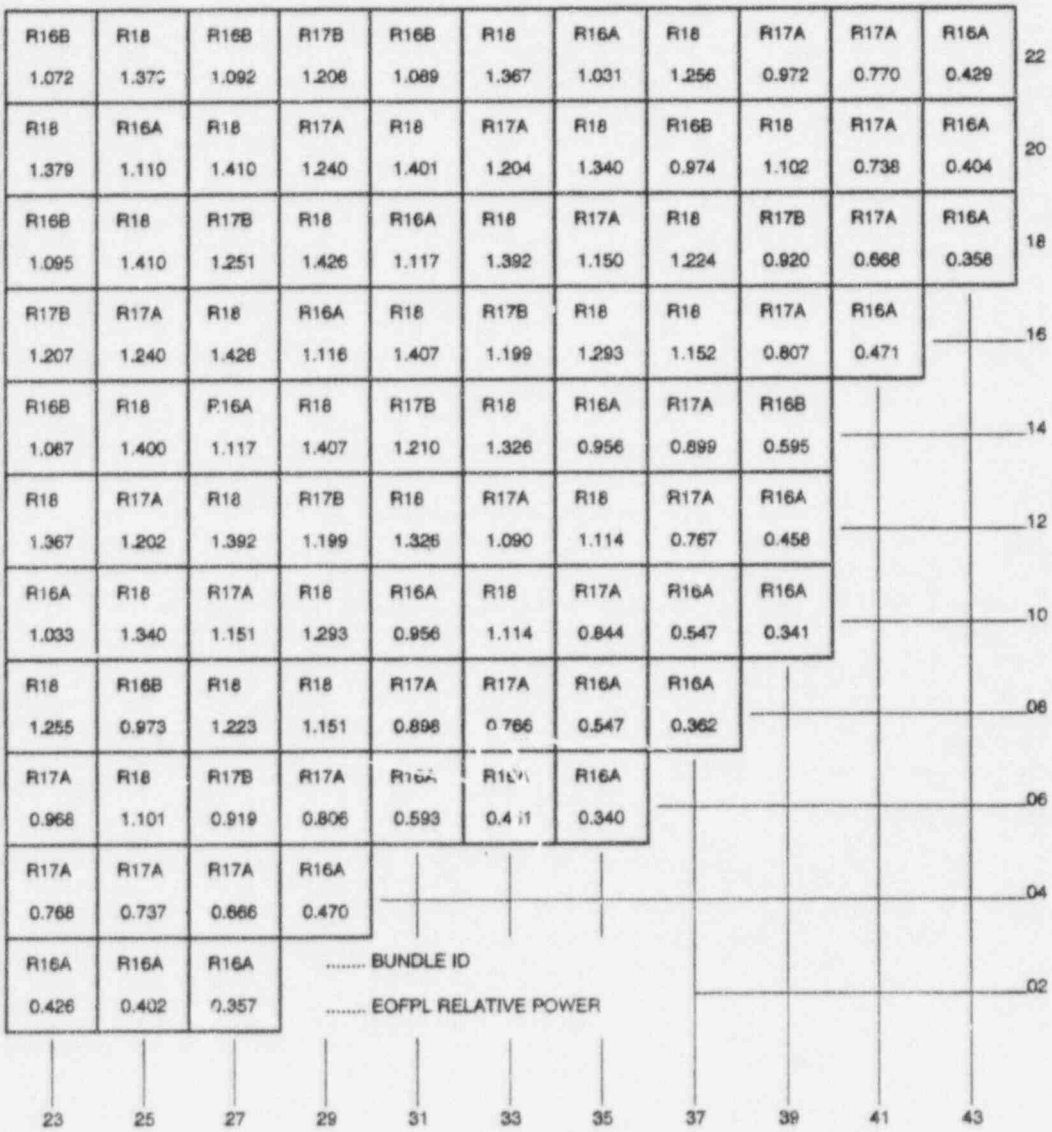

FIGURE 5.1.1

VY CYCLE 19 HALING DEPLETION,
EOFPL BUNDLE AVERAGE RELATIVE POWERS

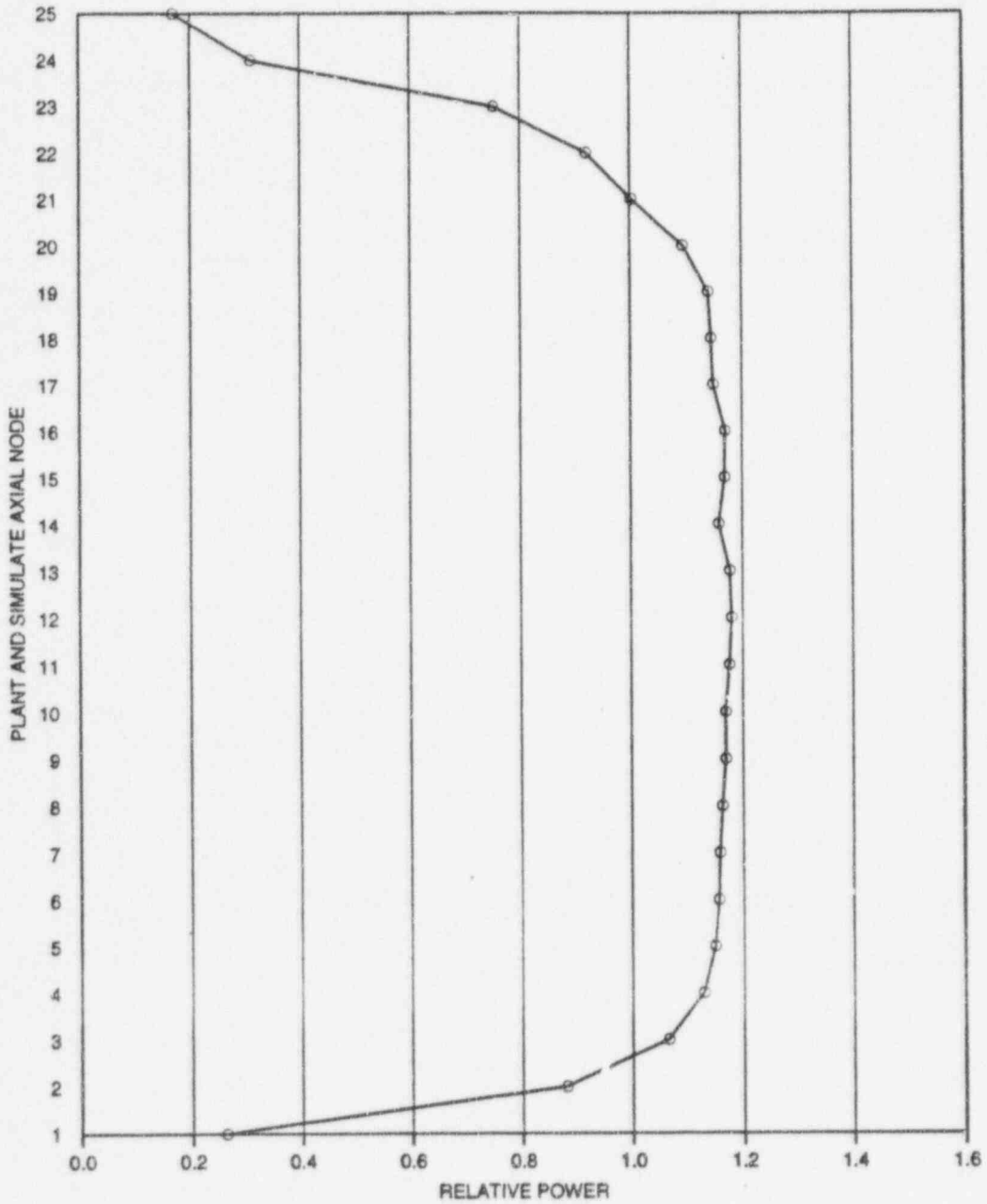

FIGURE 5.1.2

VY CYCLE 19 HALING DEPLETION, EOFPL CORE AVERAGE AXIAL POWER DISTRIBUTION

FIGURE 5.1.3

VY CYCLE 19 RODDED DEPLETION - ARO AT EOFPL,
BUNDLE AVERAGE RELATIVE POWERS

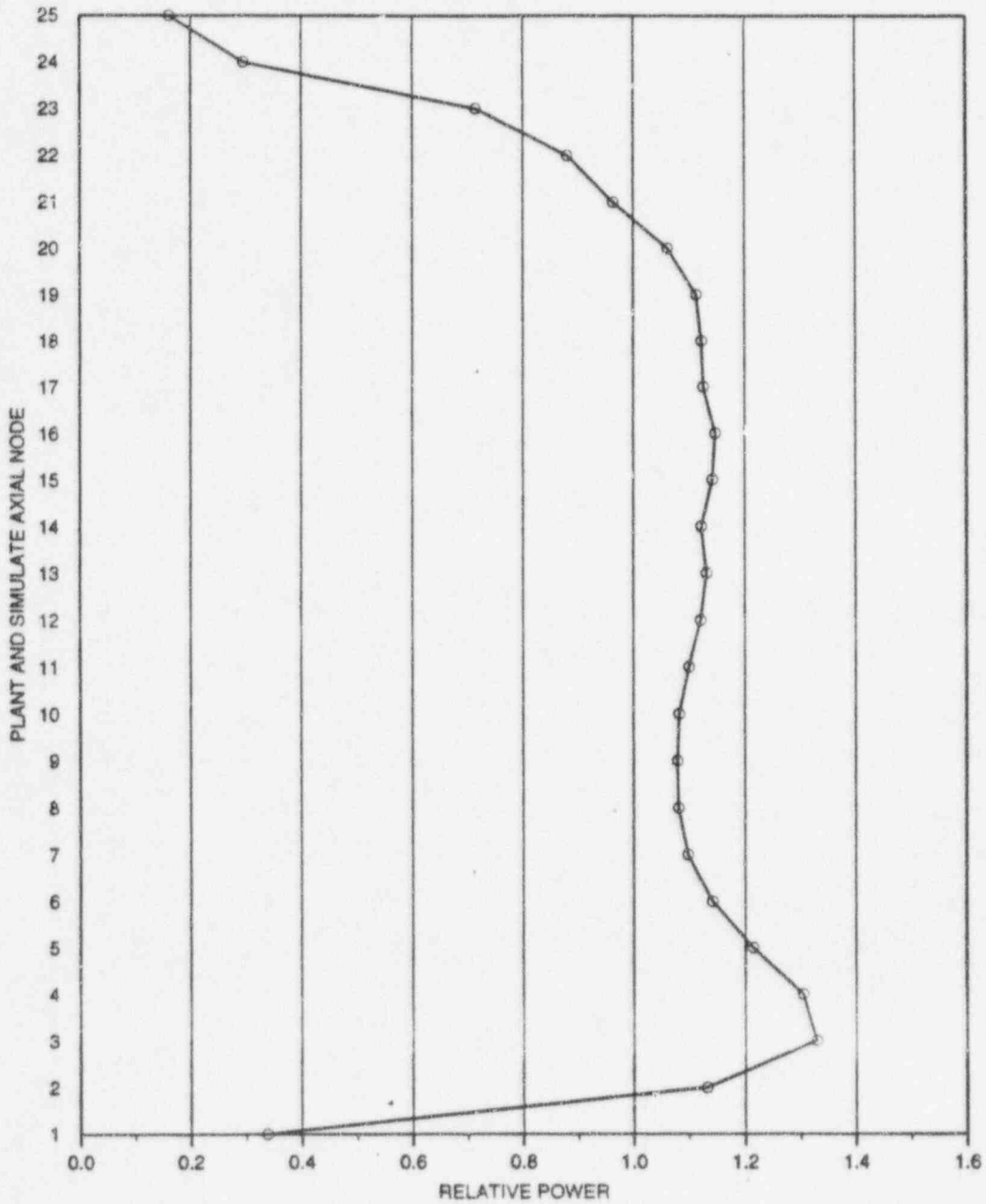

FIGURE 5.1.4

VY CYCLE 19 RODDED DEPLETION - ARO AT EOFPL,
CORE AVERAGE AXIAL POWER DISTRIBUTION

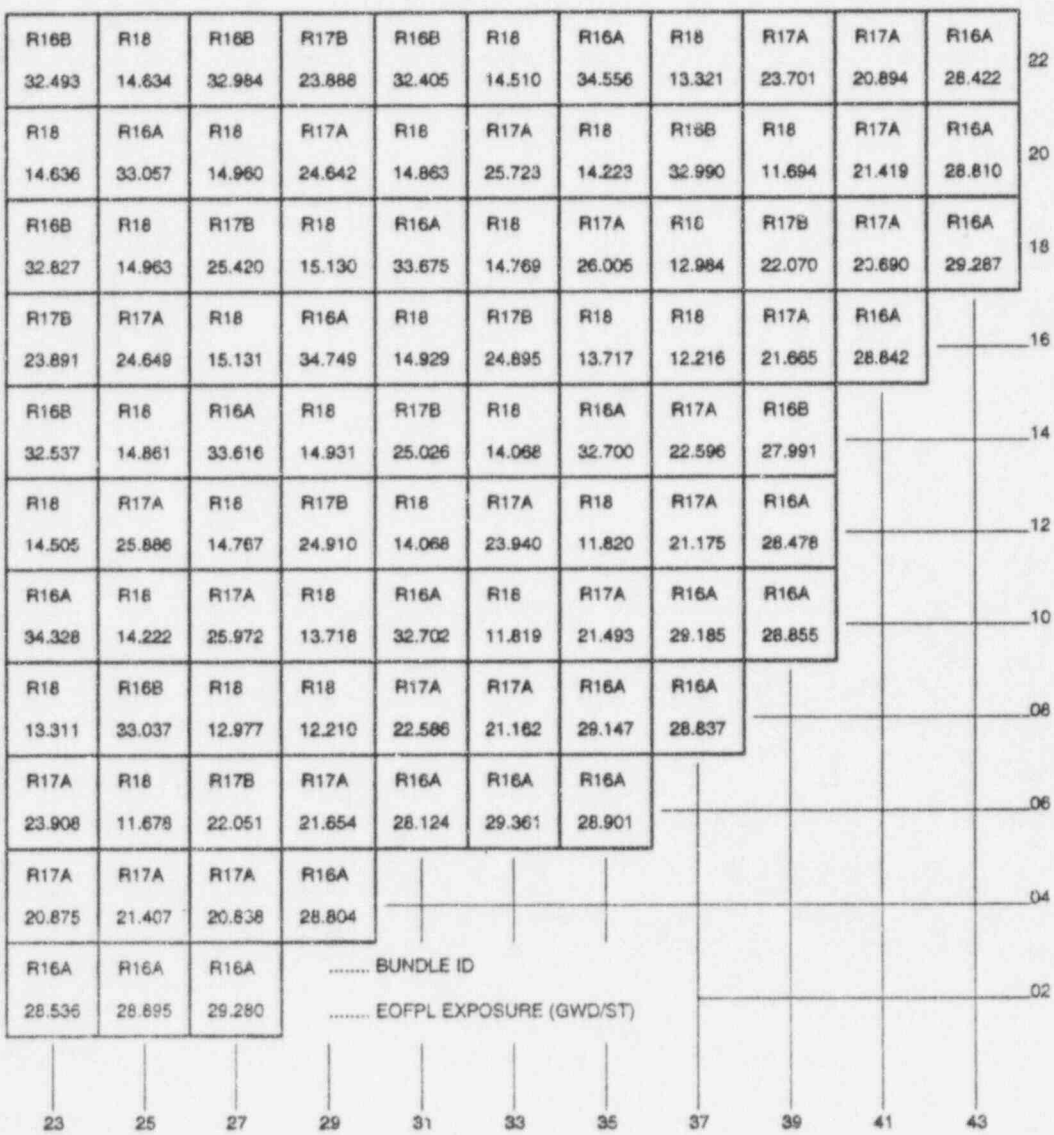

FIGURE 5.2.1

VY CYCLE 19 HALING DEPLETION, EOFPL BUNDLE AVERAGE EXPOSURES

FIGURE 5.2.2

VY CYCLE 16 RODDED DEPLETION, EOFPL BUNDLE AVERAGE EXPOSURES

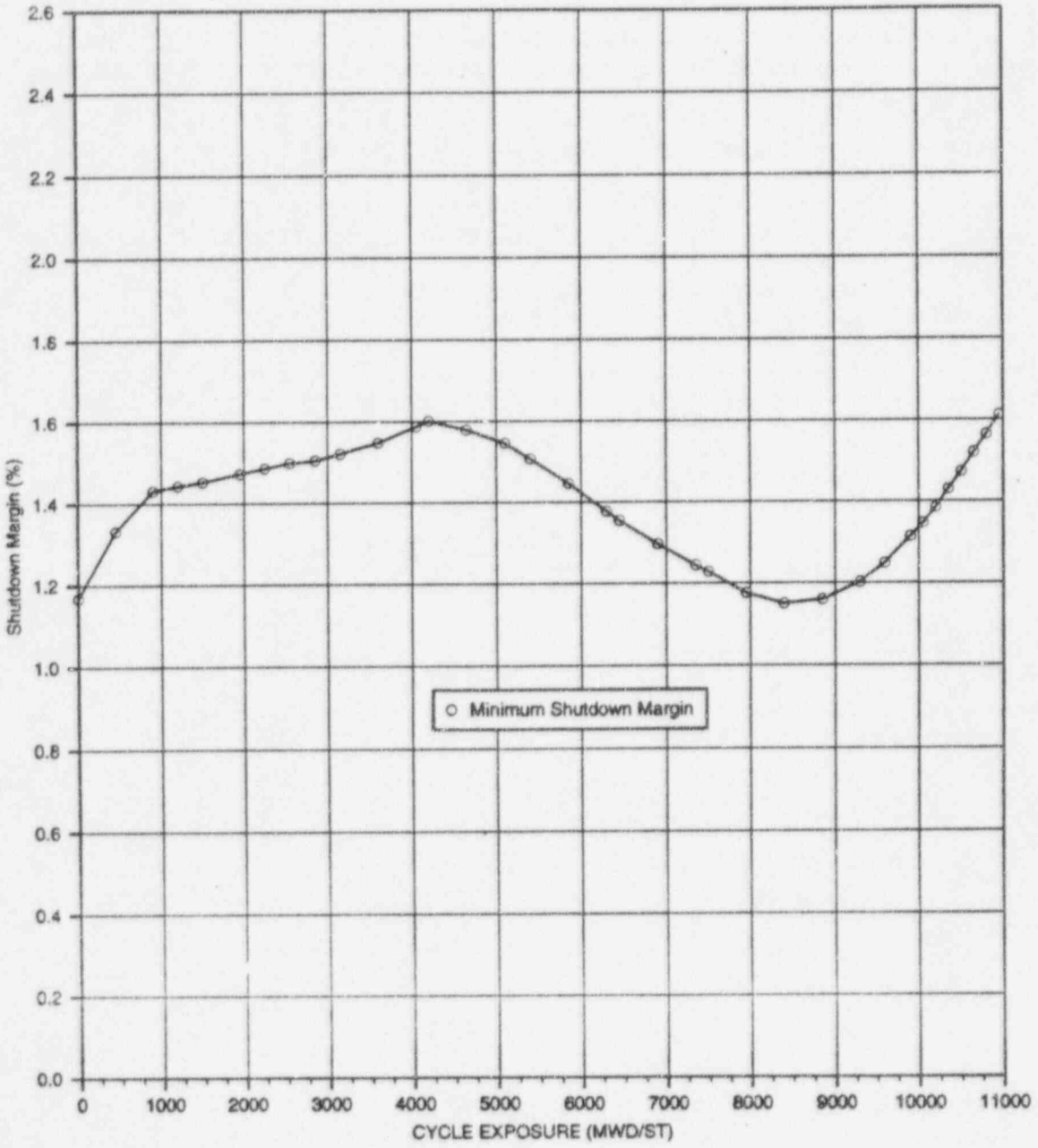

FIGURE 5.3.1

VY CYCLE 19 COLD SHUTDOWN MARGIN, IN %ΔK, VERSUS CYCLE EXPOSURE

6.0 THERMAL-HYDRAULIC DESIGN

6.1 Steady-State Thermal Hydraulics

Core steady-state thermal-hydraulic analyses for the Reload Cycle were performed using the FIBWR computer code[14],[15],[16]. The FIBWR code incorporates a detailed geometrical representation of the complex flow paths in a BWR core, and explicitly models the leakage flow to the bypass region and water rod flow. The FIBWR geometric models for each GE bundle type were benchmarked against vendor-supplied and plant thermal-hydraulic information.

Using the fuel bundle geometric models, a power distribution calculated by SIMULATE-3 and core inlet enthalpy, the FIBWR code calculates the core pressure drop and total bypass flow for several power and flow combinations. The core pressure drop and total bypass flow predicted by the FIBWR code were then used in setting the initial conditions for the system transient analysis model.

6.2 Reactor Limits Determination

Section 3.11 of the Technical Specifications requires that the plant assure the performance of the fuel rods by not exceeding the Minimum Critical Power Ratio (MCPR), the Maximum Linear Heat Generation Rate (MLHGR), and the Maximum Average Planar Linear Heat Generation Rate (MAPLHGR).

The Reload Cycle fuel has the MCPR operating limits shown in Appendix A. The MCPR is a combination of the Fuel Cladding Integrity Safety Limit (FCISL) and the change in a Critical Power Ratio (ΔCPR) which occurs during an anticipated operational transient. For Vermont Yankee, the FCISL, or commonly called the Safety Limit MCPR, is 1.10 for two loop operation or 1.12 for single loop operation [17],[18]. CPR is defined as the ratio of the critical power (bundle power at which some point within the assembly experiences onset of boiling transition) to the operating bundle power. The objective for normal operation and anticipated transient events is to maintain nucleate boiling. Avoiding a transition to film boiling protects the fuel cladding integrity. Both the transient and normal MCPR operating limits are derived with the GEXL-Plus correlation[19], with appropriate coefficients representative of the Reload Cycle's fuel types. For core flows other than rated, the MCPR limits must

be adjusted by a generic factor, K_f [19]. The analysis, described in the Section 7.0, determines the Reload Cycle MCPR operating limits.

The Reload Cycle fuel has a Linear Heat Generation Rate (LHGR) limit of 14.4 kW/ft for all bundle types. The basis for this limit can be found in Reference 2.

The Reload Cycle fuel has Average Planar Linear Heat Generation Rate (APLHGR) limits, shown in Appendix A. The Maximum APLHGR (MAPLHGR) values are the most limiting of the fuel rod thermal-mechanical MAPLHGRs [20] and the LOCA analysis MAPLHGRs (Section 8.2). The fuel rod thermal-mechanical MAPLHGRs are the result of the GE fuel rod thermal-mechanical design analyses, described in Reference 2. These results assume that during steady-state: 1) the maximum LHGR is 14.4 kW/ft, 2) the maximum peak pellet exposure is 60.0 GWd/Mt, and 3) maximum operating time is 7.0 years. These results also assume that, during an anticipated operational transient, the thermal and mechanical overpower limits [21] are not exceeded. The transient analysis, described in Section 7.0, assures that the thermal and mechanical overpower limits are not exceeded. The LOCA analysis, described in Section 8.0, determines the LOCA analysis MAPLHGRs.

7.0 ABNORMAL OPERATIONAL TRANSIENT ANALYSIS

7.1 Transients Analyzed

Transient simulations are performed to assess the impact of certain transients on the heat transfer characteristics of the fuel. The purpose of this analysis is: 1) to determine the MCPR operating limit so that the FCISL is not violated for the transients considered, 2) to assure that the thermal and mechanical overpower limits are not exceeded during the transient, 3) to demonstrate compliance with the ASME vessel code limits and 4) to assure a pressure margin greater than 25 psi below the safety valve actuation settings.

Past licensing analyses have shown that these transients impact the operating MCPR limit:

1. Pressurization transients, including the generator load rejection with complete failure of the turbine bypass system and the turbine trip with complete failure of the turbine bypass system;

2. Loss of feedwater heating, including the loss of a feedwater heater and loss of stator cooling;

3. Continuous Rod Withdrawal During Power Range Operation or commonly called the local rod withdrawal error; and

4. Fuel assembly insertion error during refueling or commonly called the misloaded bundle error including the rotated bundle error and the mislocated bundle error.

To demonstrate that the fuel rod thermal and mechanical overpowers are not exceeded, the maximum powers resulting from the pressurization, loss of feedwater heating and rod withdrawal error transients were compared to the criteria. To demonstrate compliance with ASME vessel code limits, the main steam isolation valves (MSIV) closing with failure of the MSIV position switch is also analyzed. To assure that there is a pressure margin greater than 25 psi below the safety valve actuation settings, a generator load rejection with complete failure of the turbine bypass system is

analyzed. To accommodate operation at 100% power with an inoperable safety relief valve (SRV), all transient analyses assume the lowest setpoint valve fails to open. Brief descriptions and the results of the transients analyzed are provided in the following sections.

7.2 Pressurization Transients Analysis

7.2.1 Methodology

The analysis involves two types of simulations. A system level simulation is performed to determine the overall plant response. Transient core inlet and exit conditions and normalized power from the system level calculation are then used to perform detailed thermal-hydraulic simulations of the fuel, referred to as "hot channel calculations." The hot channel simulations provide the bundle transient ΔCPR (the initial bundle CPR minus the MCPR experienced during the transient).

The system level simulations are performed with the one dimensional (1-D) kinetics RETRAN model [22],[23],[24]. The hot channel calculations are performed with the RETRAN [25],[26] and TCPYA01[27],[16],[23] computer codes. The GEXL-Plus correlation [19], contained in TCPYA01, evaluates the transient critical power ratio.

The hot channel transient ΔCPR calculations employ a two-part process, as illustrated by the flow chart in Figure 7.2.1. The first part involves a series of steady-state analyses performed with the FIBWR, RETRAN, and TCPYA01 computer codes. The FIBWR analyses utilize a one-channel model for each fuel type being analyzed, with bypass and water rod flow also modeled. The steady-state FIBWR analyses were performed at several power levels with other conditions (i.e., core pressure drop, system pressure, and core inlet enthalpy) held constant. The FIBWR code results provide a steady-state CPR, active channel flow (AF) and bypass flow (BPF) for each active channel power (AP).

The FIBWR conditions for channel power, channel flow, and bypass flow were then used as input to steady-state RETRAN/TCPYA01 hot channel calculations. Other assumptions are consistent with those in the FIBWR analysis. The Initial Critical Power Ratio (ICPR) is the result of the steady-state RETRAN/TCPYA01 analysis. These results allow for the development of functional

relationships, describing AP as a function of ICPR, and AF and BPF as functions of AP for each fuel type. These relationships are used in the iterative process for determining the transient CPR, as shown in Figure 7.2.1.

The second part of the hot channel calculations determines the transient CPR performance. Because the ΔCPR for a given transient varies with Initial Critical Power Ratio (ICPR), the hot channel analysis is an iterative process. The objective of the hot channel iteration for each transient is to determine the hot channel initial conditions which result in reaching the FCISL. Each iteration requires a RETRAN hot channel run to calculate the transient enthalpies, flows, pressure and saturation properties at each time step. These are required for input to the TCPYA01 code. TCPYA01 is then used to calculate a CPR at each time step during the transient, from which a transient ΔCPR is derived.

In response to the NRC Safety Evaluation for FROSSTEY-2 [9], the hot channel methodology has considered the assumption of both fixed and time-varying power shapes. The fixed power shape assumes a 1.4 chopped cosine axial distribution which remains constant throughout the transient. The initial power shape for the time-varying power shape methodology is the Haling axial distribution used in the core wide analysis. The time-varying hot channel power distribution is assumed to be the same as that in the core wide analysis to account for the effects of transient power feedbacks and the scram. The transient MCPR limits are defined as the more conservative results from the fixed and varying shape analyses.

7.2.2 Initial Conditions and Assumptions

The initial conditions for the Reload Cycle are based on a reactor power level of 1664 MW_{th} which includes a 4.5% margin on the current licensed reactor power level of 1593 MW_{th}. This margin conservatively bounds the expected 2% calorimetric uncertainty. The reactor core flow is assumed to be 100% of rated. The core axial power distribution for each of the exposure points is based on the 3-dimensional SIMULATE-3 predictions associated with the generation of the reactivity data (Section 7.2.3). The core inlet enthalpy is set so that the amount of carry under from the steam separators and the quality in the liquid region outside the separators is as close to zero as possible. For fast pressurization transients, this maximizes the initial pressurization rate and results in a more severe

neutron power spike. A summary of the initial operating state used for the system simulations is provided in Table 7.2.1.

During the cycle, Vermont Yankee can adjust the core flow to account for reactivity changes rather than using the control rods. During this type of operation, core flow may be as low as 87% while at 100% power. To ensure the safety analysis bounds these conditions, transients are also analyzed at the limiting exposure statepoint at 1664 MW_{th} power and 87% flow. Limiting exposure is defined as the exposure which had the highest ΔCPR.

Assumptions specific to a particular transient are discussed in the section describing the transient. In general, the following assumptions are made for all transients:

1. Scram setpoints are at Technical Specification [10] limits.

2. Protective system logic delays are at equipment specification limits.

3. Safety/relief valve and safety valve capacities are based on Technical Specification rated values.

4. Safety/relief valve (SRV) and safety valve (SV) setpoints are modeled as being at the Technical Specification setpoint plus 3%. Valve responses are based on slowest specified response values. One inoperable SRV is assumed in the analysis.

5. Control rod drive scram speed is based on the Technical Specification limits, except for the notch position 46 which is assumed to have a scram speed of 0.5 seconds. The analysis addresses a dual set of scram speeds, referred to as the "Measured" and the "67B" scram times. "Measured" refers to the faster scram times given in Section 3.3.C.1.1 of the Technical Specifications. "67B" refers to the slower scram times given in Technical Specifications 3.3.C.1.2.

7.2.3 One-Dimensional Cross Sections and Kinetics Parameters

The one-dimensional (1-D) cross sections and kinetics parameters are generated as functions of fuel temperature, moderator density, and scram. The method [28] is outlined below.

A complete set of 1-D cross sections, kinetics parameters, and axial power distributions are generated from base states using the Haling depletion established for EOFPL, EOFPL-1000 MWd/St, EOFPL-2000 MWd/St, and BOC exposure statepoints. These statepoints are characterized by exposure and void history distributions, control rod patterns, and core thermal-hydraulic conditions. The latter are consistent with the assumed system transient conditions provided in Table 7.2.1.

The BOC base state is established by shuffling from the previously defined Current Cycle endpoint into the Reload Cycle loading pattern. A criticality search provides an estimate of the BOC critical rod pattern. The EOFPL and intermediate core exposure and void history distributions are calculated with a Haling depletion as described in Section 5.2. The EOFPL state is unrodded. The EOFPL-1000 MWd/St and EOFPL-2000 MWd/St exposure statepoints require base control rod patterns. These are developed to be as "black and white" as possible to minimize the scram reactivity, maximize the core average moderator density reactivity coefficient and, therefore, maximize the transient power response. Beginning with the rodded depletion configuration, all control rods which are more than half inserted are fully inserted, and all control rods which are less than half inserted are fully withdrawn. If the SIMULATE-3 calculated parameters are within operating limits, then this configuration becomes the base case. If the limits are exceeded, a minimum number of control rods are adjusted a minimum number of notches until the parameters fall within limits.

At each exposure statepoint, a SIMULATE-3 initial control state reference case is run. A series of perturbation cases are run with SIMULATE-3 to independently vary the fuel temperature, moderator temperature, and core pressure. All other variables normally associated with the SIMULATE-3 cross sections are held constant at the reference state. To obtain the effect of the control rod scram, another SIMULATE-3 reference case is run with all-rods-in. The perturbation cases described above are run again from this reference case. For each control state, a data set of kinetics parameters and cross sections is generated as a function of the perturbed variable. There is a table set

for each of the 27 neutronic regions, 25 regions to represent the active core and one region each for the bottom and top reflectors.

7.2.4 Turbine Trip Without Bypass Transient (TTWOBP)

The transient is initiated by a rapid closure (0.1 second closing time) of the turbine stop valves. It is assumed that the steam bypass valves, which normally open to relieve pressure, remain closed. A reactor protection system signal is generated by the turbine stop valve closure switches. Control rod drive motion is conservatively assumed to occur 0.27 seconds after the start of turbine stop valve motion. The ATWS recirculation pump trip is assumed to occur at a setpoint of 1150 psig dome pressure. A pump trip time delay of 1.0 second is assumed to account for logic delay and M-G set generator field collapse. In simulating the transient, the bypass piping volume up to the valve chest is lumped into the control volume upstream of the turbine stop valves. Predictions of the salient system parameters at the three exposure points are shown in Figures 7.2.2 through 7.2.4 for the "Measured" scram time analysis.

7.2.5 Generator Load Rejection Without Bypass Transient (GLRWOBP)

The transient is initiated by a rapid closure (0.3 seconds closing time) of the turbine control valves. As in the case of the turbine trip transient, the bypass valves are assumed to fail. A reactor protection system signal is generated by the hydraulic fluid pressure switches in the acceleration relay of the turbine control system. Control rod drive motion is conservatively assumed to occur 0.28 seconds after the start of turbine control valve motion. The same modeling regarding the ATWS pump trip and bypass piping is used as in the turbine trip simulation. The influence of the accelerating main turbine generator on the recirculation system is simulated by specifying the main turbine generator electrical frequency as a function of time for the M-G set drive motors. The main turbine generator frequency curve is based on a 100% power plant startup test and is considered representative for the simulation. The system model predictions for the three exposure points are shown in Figures 7.2.5 through 7.2.7 for the "Measured" scram time analysis.

7.2.6 Pressurization Transient Analysis Results

The transients selected for consideration were analyzed at exposure points of EOFPL, EOFPL-1000 MWd/St, and EOFPL-2000 MWd/St. The MCPR limits, in Table 7.2.2, are calculated by adding the calculated ΔCPR to the FCISL for the limiting bundle type in the core. The worst ΔCPR for the pressurization transients account for an exposure window of 0.0 to +600 MWd/St on Current Cycle and its impact on the Reload Cycle [7]. The fuel rod thermal and mechanical overpowers are not exceeded for these transients.

7.3 Loss of Feedwater Heating Transient Analysis

7.3.1 Loss of a Feedwater Heater (LOFWH) Results

A feedwater heater can be lost in such a way that the steam extraction line to the heater is shut off or the feedwater flow bypasses one of the heaters. In either case, the reactor will receive cooler feedwater, which will produce an increase in the core inlet subcooling, resulting in a reactor power increase.

The response of the system due to the loss of 100°F of the feedwater heating capability was analyzed. This represents the maximum expected feedwater temperature reduction for a single heater or group of heaters that can be tripped or bypassed by a single event. The system model used is the same as that used for the pressurization transient analysis (Section 7.2.1). The initial conditions and modeling assumptions discussed in Section 7.2.2 are applicable to this simulation.

Vermont Yankee has a scram setpoint of 120% of rated power as part of the Reactor Protection System (RPS) on high neutron flux. In this analysis, no credit was taken for scram on high neutron flux, thereby allowing the reactor power to reach its peak without scram. This approach was selected to provide a bounding and conservative analysis for events initiated from any power level.

The transient response of the system was evaluated at several exposures during the cycle, EOFPL, EOFPL-1000 MWd/St, EOFPL-2000 MWd/St, and BOC. The transient results, corresponding to the limiting bundle type in the core, are listed in Table 7.3.1. The MCPR limits in

Table 7.3.1 are calculated by adding the calculated ΔCPR to the FCISL. The transient evaluation at EOFPL was found to be the limiting case. The results of the system response to a loss of 100°F feedwater heating capability evaluated at EOFPL, as predicted by the RETRAN code, are presented in Figure 7.3.1. The fuel rod thermal and mechanical overpowers are not exceeded for this transient.

7.3.2 Loss of Stator Cooling (LOSC) Results

In response to a loss of stator cooling, a turbine runback is initiated to reduce generator output to less than 29% of rated output. This runback is accomplished by bypassing main steam from the turbine directly to the main condenser. Since heating steam to the feedwater heaters is supplied from the turbine stages, the amount of steam available for feedwater heating is significantly reduced. The reduction of heating steam to the feedwater heaters results in a severe subcooling event.

For the analysis, the loss of stator cooling event is initiated at, or near, rated thermal power (maximum 104.5%). It is assumed that an instantaneous loss of extraction steam occurs to the Nos. 1-4 feedwater heaters of both feedwater trains. This is a conservative assumption, since there would not be a total loss of steam to the feedwater heaters, and the reduction in heating steam would occur over the several minutes required for the turbine runback. Also, no credit is taken for the heat capacity of structural materials in the process piping or feedwater heaters. This results in a stepwise decrease in feedwater inlet temperature as the feedwater travels through the feedwater piping to the reactor vessel.

The decrease in feedwater temperature results in a subsequent reduction in core inlet temperature. Due to the negative void coefficient, core thermal power increases. The transient is terminated by APRM high flux trip at 120% of rated core thermal power.

The transient response of the system was evaluated at several exposures during the cycle, EOFPL, EOFPL-1000 MWd/St, EOFPL-2000 MWd/St, and BOC. The transient results, corresponding to the limiting bundle type in the core, are listed in Table 7.3.2. The MCPR limits in Table 7.3.2 are calculated by adding the calculated ΔCPR to the FCISL. The transient evaluation at several exposures, including EOFPL, were found to be limiting. The results of the system response to a loss of stator cooling evaluated at EOFPL, as predicted by the RETRAN code, are presented in Figure 7.3.2 as an

example. To assure that the thermal overpower limits are not exceeded, the MAPLHGR limits were modified.

7.4 Overpressurization Analysis Results

7.4.1 Compliance with ASME Vessel Code

Compliance with ASME vessel code limits is demonstrated by an analysis of the Main Steam Isolation Valves (MSIV) closing with failure of the MSIV position switch scram. EOFPL conditions were analyzed. The system model used is the same as that used for the transient analysis (Section 7.2.1). The initial conditions and modeling assumptions discussed in Section 7.2.2 are applicable to this simulation.

The transient is initiated by a simultaneous closure of all MSIVs. A 3.0 second closing time, which is the minimum time in Technical Specification Table 4.7.2, is assumed. A reactor scram signal is generated on APRM high flux. Control rod drive motion is conservatively assumed to initiate 0.28 seconds after reaching the high flux setpoint. One safety relief valve (SRV) is assumed to be inoperable. The system response is shown in Figure 7.4.1 for the "67B" scram time analysis.

The maximum pressures at the bottom of the reactor vessel calculated for the "67B" scram time analysis are given in Table 7.4.1. These results are within the ASME code overpressure design limit which is 110% of the vessel design pressure. Vermont Yankee's design pressure is 1250 psig so the maximum pressure limit is 1375 psig.

7.4.2 Safety Valve Challenges

An overpressure analysis was performed to assure that sufficient pressure margin exists below the safety valve setpoint with one inoperable SRV during the limiting AOT. For this purpose, the limiting AOT for the Reload Cycle is the GLRWOBP at EOFPL conditions. The system model used is the same as that used for the transient analysis (Section 7.2.1). The transient scenario is the same as described in Section 7.2.5. The analysis is typically performed with best estimate assumptions. However, this analysis was performed with the following conservative assumptions:

1) the same power and flow conditions described in Section 7.2.2,

2) an inoperable SRV,

3) all of the SRVs opening setpoint was assumed to have drifted up to 1110 psig (1% above 1100),

4) the safety valves opening setpoint was assumed to have drifted down to 1227.6 psig (1% below 1240 psig), and

5) the "Measured" scram insertion times.

The acceptance criteria for this event is a pressure margin of greater than 25 psi to the safety valve setpoint. The results are greater than 25 psi as shown in Table 7.4.2. In conclusion, operation at full power with an inoperable SRV will not cause Safety Valve challenges during an AOT.

7.5 Local Rod Withdrawal Error Transient Results

The rod withdrawal error (RWE) is a local core transient caused by an operator erroneously withdrawing a control rod in the continuous withdrawal mode. If the core is operating at its MCPR operating limit at the time of the error, the continuous withdrawal of a control rod could increase both local and core average power levels with the potential for overheating the fuel. The consequences of the error depend on the local and overall core power increases, the initial MCPRs found in locations close to the error rod, and the ability of the Rod Block Monitor (RBM) System to stop the withdrawal of the rod before MCPR reaches the FCISL.

The purpose of this analysis is to develop a MCPR operating limit for the RWE, defined at each RBM setpoint, so that the FCISL is not violated. A broad spectrum of core conditions and rod patterns can exist at the time of such an error. This analysis evaluates the RWE, as initiated from all the "normal" rod patterns and power conditions, as defined in the rodded depletion (Section 5.1.2). In addition, a significant number of "abnormal" control rod patterns and initial conditions are developed and analyzed. These abnormal cases serve the purpose of exaggerating the worth and ΔCPR impact of the error rod to be withdrawn, especially at the higher RBM setpoints.

The analysis for a given statepoint is performed using SIMULATE-3 in a quasi-static mode. the xenon distribution is held fixed at the initial state, but void and power distributions are

allowed to equilibrate at each new control rod withdrawal position during the transient. A power search increases the core average power in the model with each withdrawal step by searching on the critical eigenvalue of the initial state.

An evaluation of the instrument response of the Rod Block Monitor (RBM) System to the rod withdrawal determines at what position the error rod is blocked. The RBM System's ability to terminate the RWE is evaluated on the following bases:

1. Technical Specifications [10] allow each of the separate RBM channels to remain operable if half, or more of the Local Power Range Monitor (LPRM) inputs on each level are operable. One RBM channel averages the inputs from the A and C levels; the other channel averages the inputs from the B and D levels. For the interior locations tested in this analysis, there are four LPRM inputs per level. Thus, there are eleven failure combinations of none, one and two completely failed LPRM strings. For each RBM channel, the instrument response as a function of error rod position is chosen to be the minimum response for these eleven LPRM string failure modes.

2. The event is analyzed separately in each of the four quadrants of the core, because of the different physical locations of the LPRM strings relative to the error rod.

3. Technical Specifications require that both RBM channels be operable during normal operation. Thus, the first channel whose response is calculated to intercept the RBM setpoint is assumed to stop the rod. To allow for control system delay times, the rod is assumed to continue moving for a minimum of two inches after the signal intercepts the RBM setpoint; the rod stops at the next available notch position.

Once the notch at which the rod stops moving is determined, the ΔCPR versus RBM setpoint can be calculated. The ΔCPR is calculated such that the implied MCPR operating limit equals the FCISL + ΔCPR. This is done by conserving the figure of merit (ΔCPR/ICPR) found in the SIMULATE-3 calculations.

As already mentioned, two types of RWE cases are evaluated -- normal and abnormal.

The normal cases are initiated from the expected rod patterns found in the rodded depletion. The normal cases have the following bases:

1. The core model is initially at full power, full flow and equilibrium xenon.

2. Every control rod sequence in the rodded depletion is examined. Within each sequence a representative pattern is chosen. All deeply inserted rods (i.e., inserted above the core mid-plane) are withdrawn in separate cases.

Numerous normal cases are analyzed, as shown in Figure 7.5.1. An envelope is drawn that encompasses the most limiting ΔCPR results of all the normal cases. For conservatism, at least 0.02 ΔCPR margin is added by the envelope to assure that exposure uncertainties in the Current Cycle and the Reload Cycle are accounted for [7]. Table 7.5.1 provides the ΔCPR versus RBM setpoint envelope for the normal cases, including the 0.02 ΔCPR uncertainty.

Figure 7.5.2 provides the envelope of the worst of the abnormal case results. The abnormal cases are run to determine the sensitivity of the analysis to power level uncertainty and rod pattern variation. The abnormal cases are developed from the worst of the normal cases by specifying the following set of concurrent worst case assumptions:

1. The abnormal initial rod patterns are developed with xenon-free conditions. The xenon-free condition and the additional control rod inventory needed to maintain criticality exaggerates the worth of the withdrawn control rod when compared to normal operation with normal xenon levels.

2. The core is modeled at 104.5% power and 100% flow.

3. The core power distribution is adjusted with the available control rods (other than the error rod) to force assemblies within the four by four array of bundles around the error rod to be as close to the operating limits as possible.

Of the many abnormal pattern cases tested, an envelope of the most limiting ΔCPR results is created by rounding-up to the closest 0.01 ΔCPR. As shown in Table 7.5.1, the ΔCPR derived from the abnormal cases envelope is important in establishing the limits at the higher RBM setpoints. The final operating MCPR limit shown in Table 7.5.1 is based on the maximum ΔCPR of both the normal cases envelope (worst + 0.02 ΔCPR), and the abnormal cases envelope. The fuel rod mechanical overpowers are not exceeded for this transient.

7.6 Misloaded Bundle Error Analysis Results

7.6.1 Rotated Bundle Error

The primary result of a bundle rotation is a large increase in local pin peaking and the associated R-factor as higher enrichment pins are placed adjacent to the surrounding wide water gaps. In addition, there may be a small increase in reactivity, depending on the exposure and void fraction states. The R-factor increase results in a CPR reduction. The objective of the analysis is to ensure that, in the worst possible rotation, the FCISL is not violated with the most limiting bundles on their operating limits.

To analyze the CPR response, rotated bundle R-factors as a function of exposure are developed by adding the largest possible ΔR-factor resulting from a rotation to the exposure dependent R-factors of the properly oriented bundles. Using these rotated bundle R-factors, the MCPR values resulting from a bundle rotation are determined using SIMULATE-3. This is done for each control rod sequence throughout the cycle. The process is repeated with the K_∞ of the limiting bundle modified slightly to account for the increase in reactivity resulting from the rotation. For each sequence, the MCPR for the properly oriented bundles is adjusted by a ratio necessary to place the corresponding rotated bundle's CPR on its FCISL. The adjusted MCPRs at each exposure is the rotated bundle operating limit for the rotated bundle error. The operating MCPR limit resulting from a rotation at any exposure is presented in Table 7.6.1.

7.6.2 Mislocated Bundle Error

Mislocating a high reactivity assembly into a region of high neutron importance results in a location of high relative assembly average power. Since the assembly is assumed to be properly oriented (not rotated), R-factors used for the mislocated bundle are the standard values for the given fuel type.

The analysis uses multiple SIMULATE-3 cases to examine the effects of explicitly mislocating every older interior assembly in a quarter core with a fresh or once-burned assembly. Because of symmetry, the results apply to the whole core. Edge bundles are not examined because they are never limiting, due to neutron leakage.

The effect of the successive mislocations is examined for every control rod sequence throughout the cycle. For each sequence, the MCPR for the properly loaded core is compared to the MCPR of the misloaded core at the misloaded location. The MCPR for the properly loaded core is adjusted by a ratio necessary to place the mislocated assembly on the FCISL. The maximum of these adjusted MCPRs is the mislocated bundle operating limit. The results of the mislocated bundle analysis are given in Table 7.6.2.

7.7 Transient Analysis Results

The results of this transient analysis has: 1) determined the MCPR operating limit so that the FCISL is not violated for the transients considered, 2) assured that the thermal and mechanical overpower limits are not exceeded during the transient, 3) demonstrated compliance with the ASME vessel code limits and 4) assured there is a pressure margin greater than 25 psi below the safety valve actuation settings.

The MCPR operating limits for the Reload Cycle are calculated by adding the calculated ΔCPR to the FCISL at each of the exposure statepoints for each transient. Table 7.7.1 lists the limiting transient for each statepoint. For an exposure interval between statepoints, the highest MCPR limit at either end is assumed to apply to the whole interval. The highest calculated MCPR limits for the Reload Cycle for each of the exposure intervals for the various scram speeds and for the various

rod block lines are provided in Appendix A. These MCPR operating limits are valid for operation of the Reload Cycle at full power up to 10701 MWd/St and for operation during coastdown beyond EOFPL.

TABLE 7.2.1

VY CYCLE 19 SUMMARY OF SYSTEM TRANSIENT MODEL
INITIAL CONDITIONS FOR TRANSIENT ANALYSES

Core Thermal Power (MW_{th})	1664.0
Turbine Steam Flow ($10^6 lb_m/hr$)	6.75
Total Core Flow ($10^6 lb_m/hr$)	48.0
Core Bypass Flow ($10^6 lb_m/hr$)*	6.28
Core Inlet Enthalpy (BTU/lb_m)	523.2
Steam Dome Pressure (psia)	1034.7
Turbine Inlet Pressure (psia)	985.7
Total Recirculation Drive Flow ($10^6 lb_m/hr$)	23.7
Core Plate Differential Pressure (psi)	20.4
Narrow Range Water Level (in.)	162.0
Average Fuel Gap Conductance	(See Section 4.2)

* Includes water rod flow.

TABLE 7.2.2

VY CYCLE 19 PRESSURIZATION TRANSIENT ANALYSIS RESULTS

Transient	Exposure Statepoint	Peak Prompt Power (Fraction of Initial Value)	Peak Average Heat Flux (Fraction of Initial Value)	ΔCPR*	Transient MCPR Limits
Turbine Trip Without Bypass, "Measured" Scram Time	EOFPL	2.88354	1.20382	0.24	1.34
	EOFPL-1000	2.38439	1.14673	0.18	1.28
	EOFPL-2000	1.80549	1.06437	0.10	1.20
Turbine Trip Without Bypass, "67B" Scram Time	EOFPL	3.21942	1.25097	0.31	1.41
	EOFPL-1000	2.84459	1.20546	0.22	1.32
	EOFPL-2000	2.23193	1.12560	0.14	1.24
Generator Load Rejection Without Bypass, "Measured" Scram Time	EOFPL	2.74082	1.17762	0.23	1.33
	EOFPL-1000	2.15236	1.10768	0.16	1.26
	EOFPL-2000	1.43162	1.01683	0.08	1.18
Generator Load Rejection Without Bypass, "67B" Scram Time	EOFPL	3.28186	1.23935	0.30	1.40
	EOFPL-1000	2.83940	1.18845	0.22	1.32
	EOFPL-2000	2.07830	1.10680	0.13	1.23

* The ΔCPR accounts for an exposure window of 0 to +600 MWd/St on the Current Cycle and its impact on the Reload Cycle [7].

TABLE 7.3.1

VY CYCLE 19 LOSS OF FEEDWATER HEATER TRANSIENT RESULTS

Transient	Exposure Statepoint	Peak Prompt Power (Fraction of Initial Value)	Peak Average Heat Flux (Fraction of Initial Value)	ΔCPR	Transient MCPR Limits
Loss of 100°F Feedwater Heating	EOFPL	1.18034	1.18159	0.15	1.25
	EOFPL-1000	1.19809	1.14579	0.12	1.22
	EOFPL-2000	1.20639	1.14546	0.12	1.22
	BOC	1.14536	1.14565	0.12	1.22

TABLE 7.3.2

VY CYCLE 19 LOSS OF STATOR COOLING TRANSIENT RESULTS

Transient	Exposure Statepoint	Peak Prompt Power (Fraction of Initial Value)	Peak Average Heat Flux (Fraction of Initial Value)	ΔCPR	Transient MCPR Limits
Loss of Stator Cooling	EOFPL	1.20089	1.18898	0.16	1.26
	EOFPL-1000	1.20100	1.18894	0.16	1.26
	EOFPL-2000	1.21592	1.11061	0.09	1.19
	BOC	1.20187	1.18756	0.16	1.26

TABLE 7.4.1

VY CYCLE 19 ASME COMPLIANCE RESULTS

Conditions	Maximum Pressure at Reactor Vessel Bottom (psig)
"67B" Scram Time	1319

TABLE 7.4.2

VY CYCLE 19 SAFETY VALVE SETPOINT CHALLENGE RESULTS

Peak Steam Line Pressure (psig)	Safety Valve Setpoint (-1%) (psig)	Margin (psi)
1190.8	1227.6	36.8

TABLE 7.5.1

VY CYCLE 19 ROD WITHDRAWAL ERROR ANALYSIS RESULTS

Rod Block Monitor Setpoint	ΔCPR Envelope from Normal Cases (Worst + 0.02)	ΔCPR Envelope from Abnormal Cases (Worst Rounded Up)	Transient MCPR Limits
104	0.11	0.10	1.21
105	0.14	0.12	1.24
106	0.16	0.13	1.26
107	0.18	0.17	1.28
108	0.19	0.22	1.32

TABLE 7.6.1

VY CYCLE 19 ROTATED BUNDLE ANALYSIS RESULTS

Transient MCPR Limit
1.29

TABLE 7.6.2

VY CYCLE 19 MISLOCATED BUNDLE ANALYSIS RESULTS

Transient MCPR Limit
1.17

TABLE 7.7.1

VY CYCLE 19 LIMITING TRANSIENTS

Rod Block Monitor Setpoint	Scram Time	Exposure (GWd/St)	Limiting Transient	Transient MCPR Limit
108	Measured	0.0 to 9.7	Rod Withdrawal Error	1.32
		9.7 to 10.7	Turbine Trip	1.34
108	"67B"	0.0 to 9.7	Rod Withdrawal Error	1.32
		9.7 to 10.7	Turbine Trip	1.41
107	Measured	0.0 to 9.7	Rotated Bundle	1.29
		9.7 to 10.7	Turbine Trip	1.34
107	"67B"	0.0 to 8.7	Rotated Bundle	1.29
		8.7 to 9.7	Turbine Trip	1.32
		9.7 to 10.7	Turbine Trip	1.41
106	Measured	0.0 to 9.7	Rotated Bundle	1.29
		9.7 to 10.7	Turbine Trip	1.34
106	"67B"	0.0 to 8.7	Rotated Bundle	1.29
		8.7 to 9.7	Turbine Trip	1.32
		9.7 to 10.7	Turbine Trip	1.41

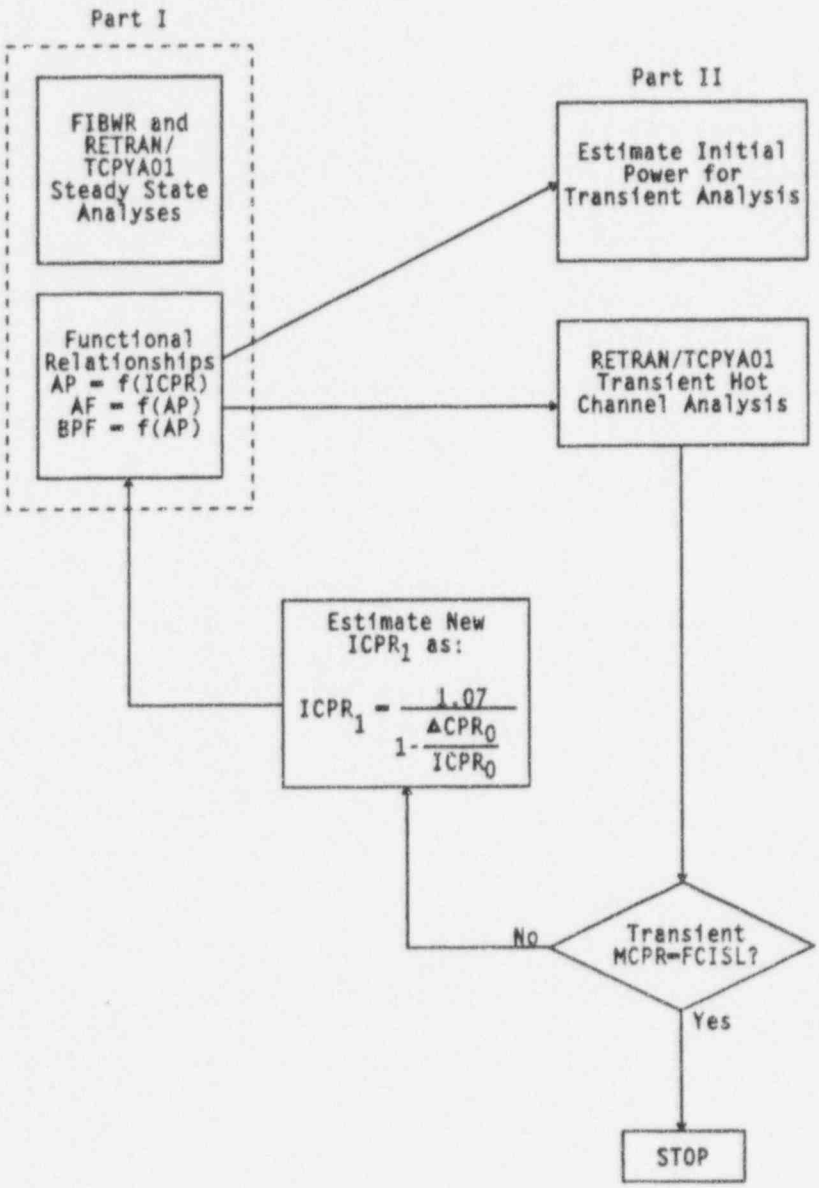

FIGURE 7.2.1

FLOW CHART FOR THE CALCULATION OF ΔCPR USING THE RETRAN/TCPYA01 CODES

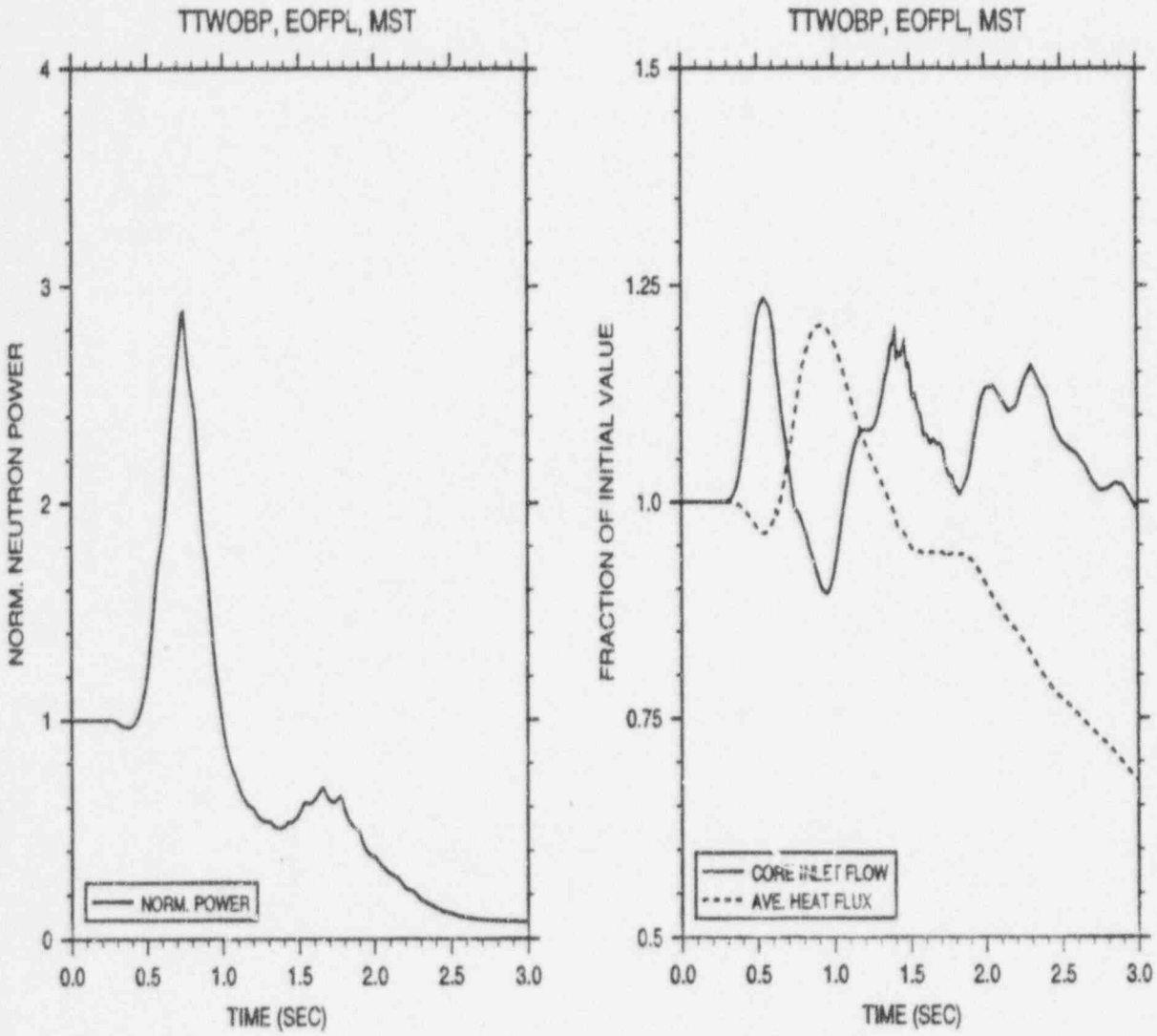

FIGURE 7.2.2

TURBINE TRIP WITHOUT BYPASS, EOFPL19
TRANSIENT RESPONSE VERSUS TIME, "MEASURED" SCRAM TIME

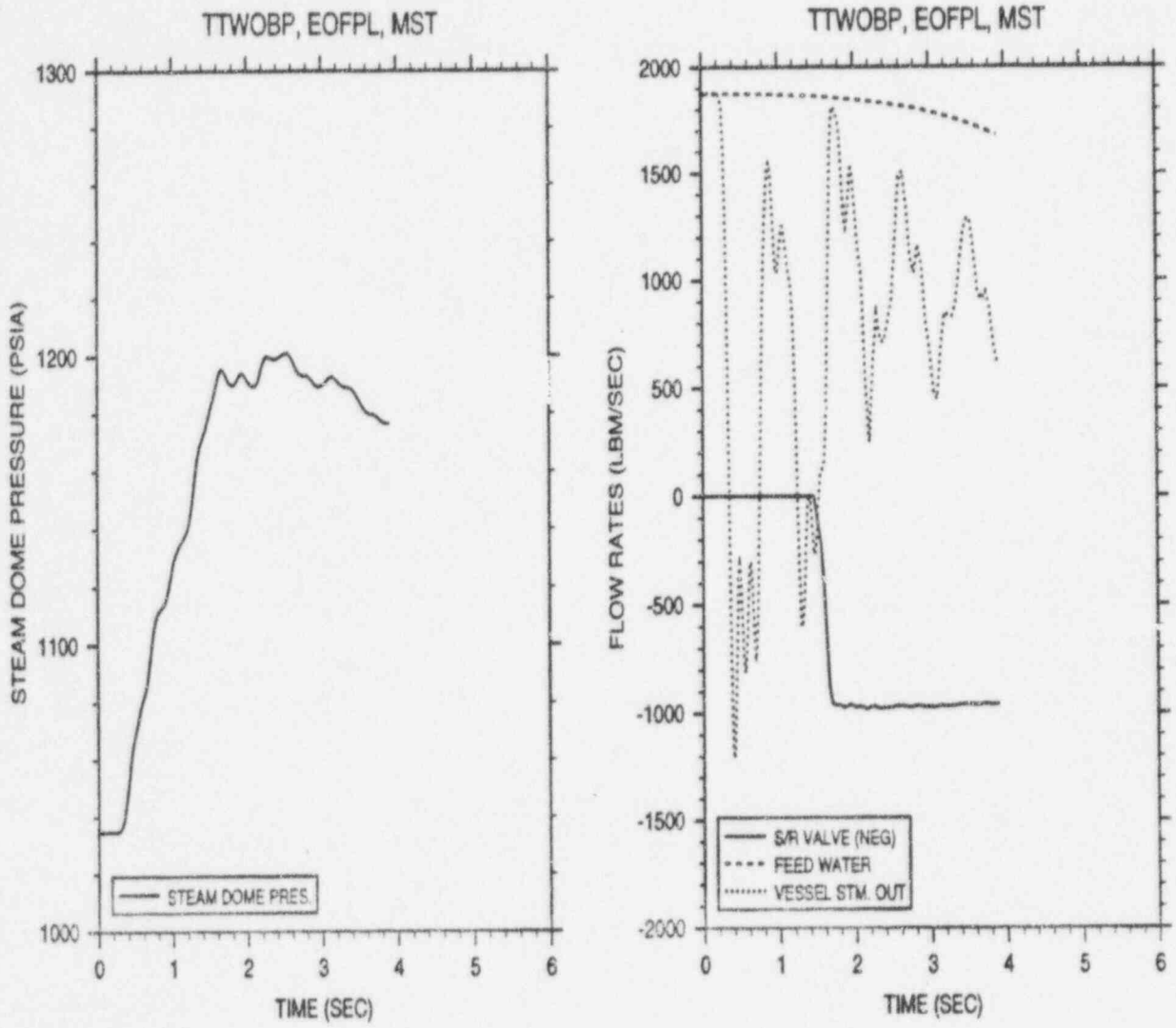

FIGURE 7.2.2
(Continued)

TURBINE TRIP WITHOUT BYPASS, EOFPL19
TRANSIENT RESPONSE VERSUS TIME, "MEASURED" SCRAM TIME

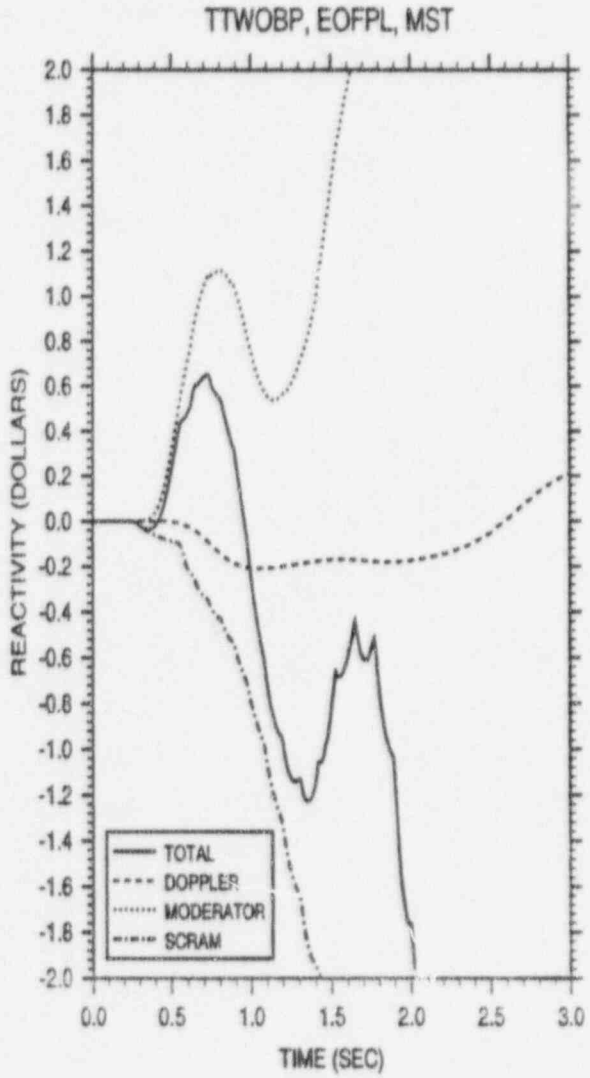

FIGURE 7.2.2
(Continued)

TURBINE TRIP WITHOUT BYPASS, EOFPL19
TRANSIENT RESPONSE VERSUS TIME, "MEASURED" SCRAM TIME

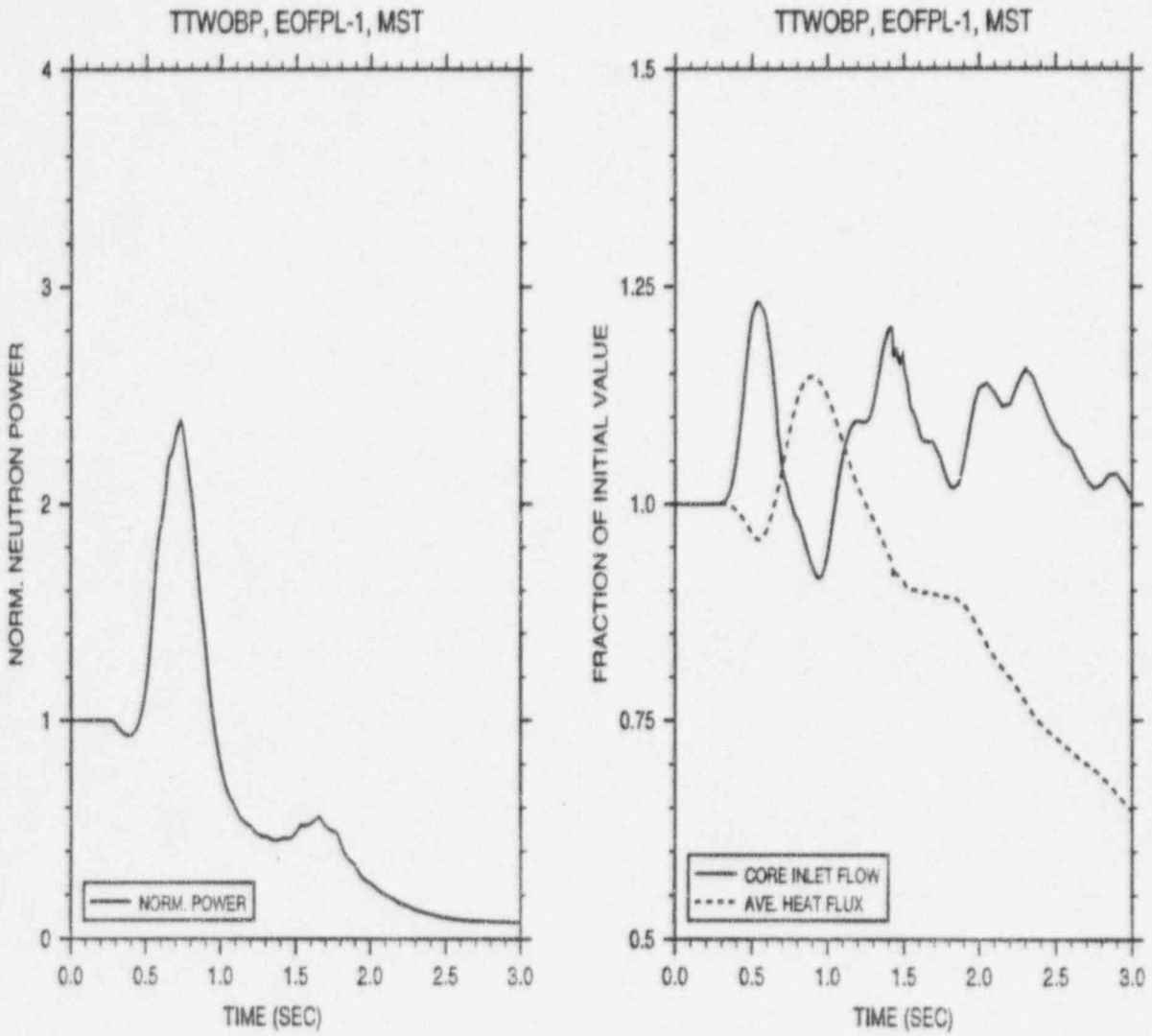

FIGURE 7.2.3

TURBINE TRIP WITHOUT BYPASS, EOFPL19-1000 MWD/ST
TRANSIENT RESPONSE VERSUS TIME, "MEASURED" SCRAM TIME

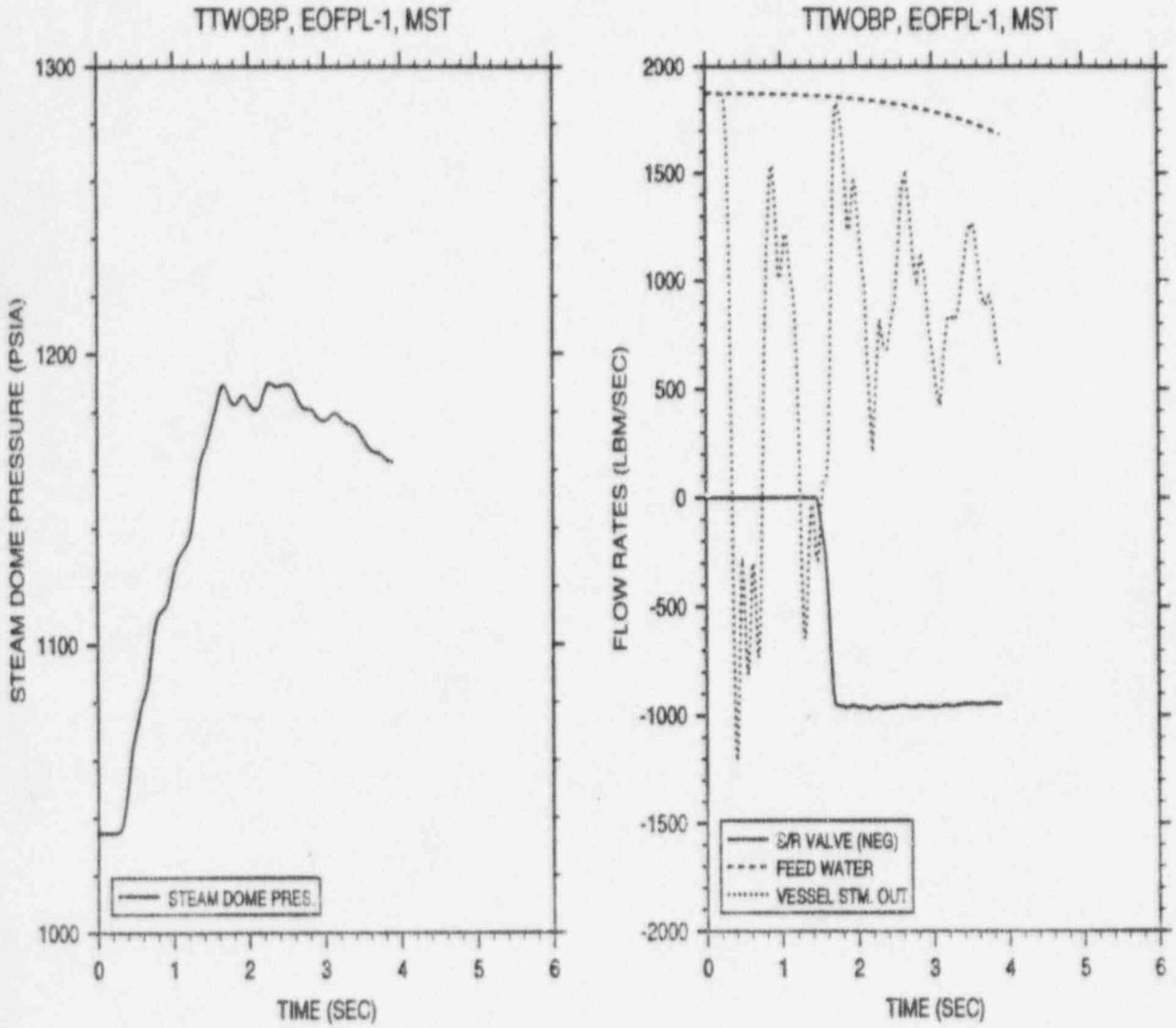

FIGURE 7.2.3
(Continued)

TURBINE TRIP WITHOUT BYPASS, EOFPL19-1000 MWD/ST
TRANSIENT RESPONSE VERSUS TIME, "MEASURED" SCRAM TIME

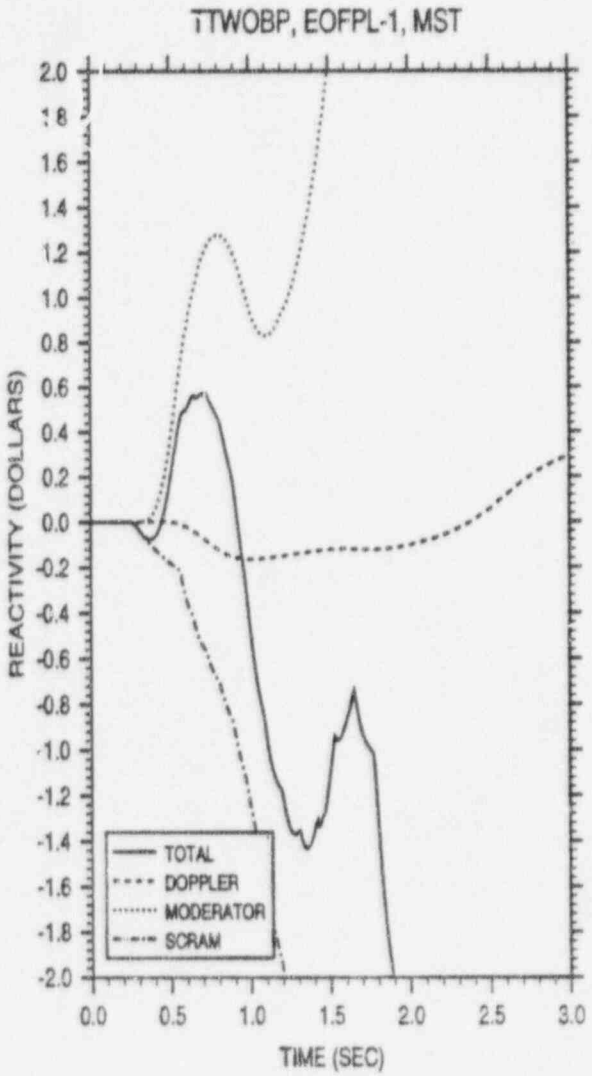

FIGURE 7.2.3
(Continued)

TURBINE TRIP WITHOUT BYPASS, EOFPL19-1000 MWD/ST
TRANSIENT RESPONSE VERSUS TIME, "MEASURED" SCRAM TIME

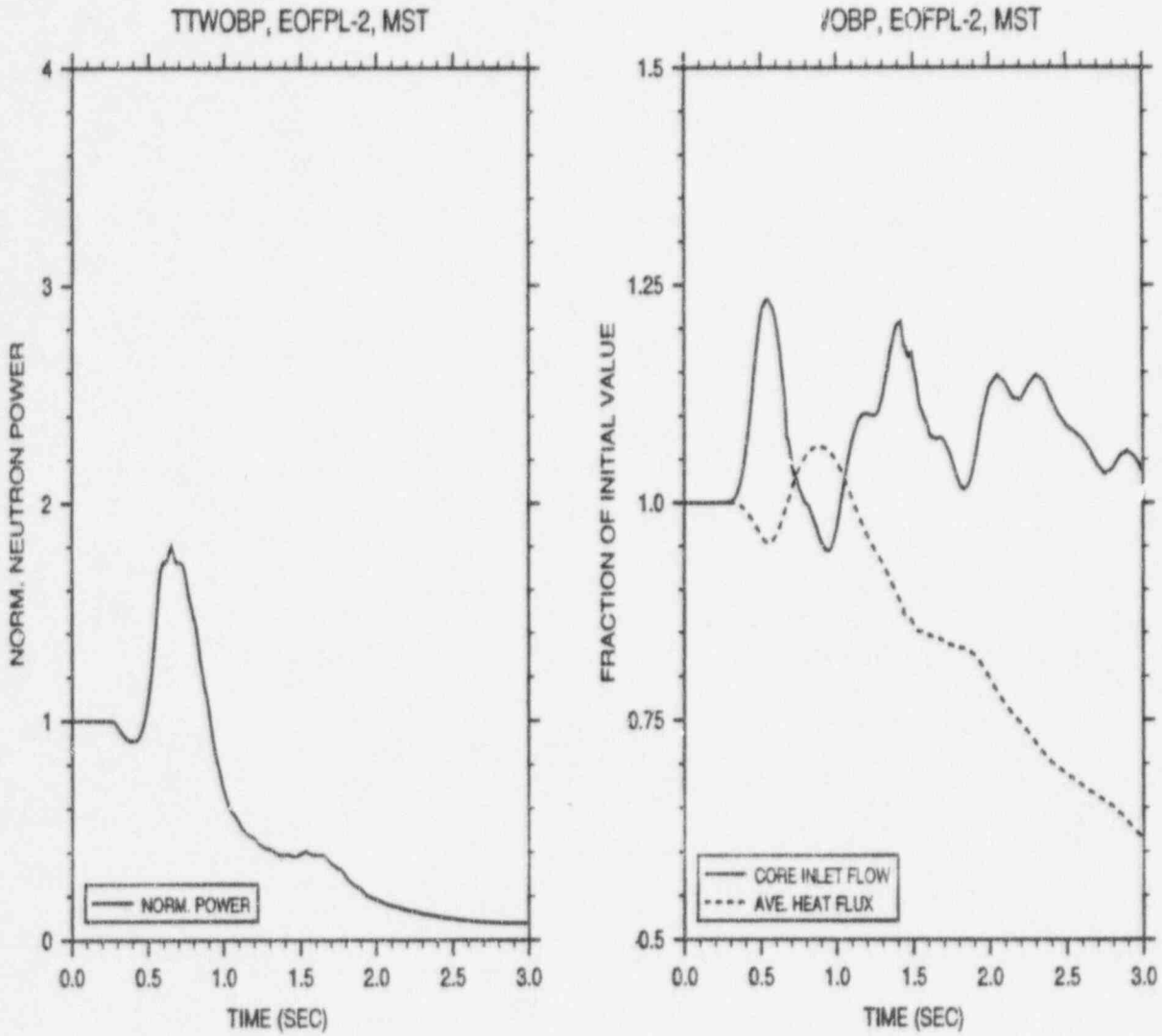

FIGURE 7.2.4

TURBINE TRIP WITHOUT BYPASS, EOFPL19-2000 MWD/ST
TRANSIENT RESPONSE VERSUS TIME, "MEASURED" SCRAM TIME

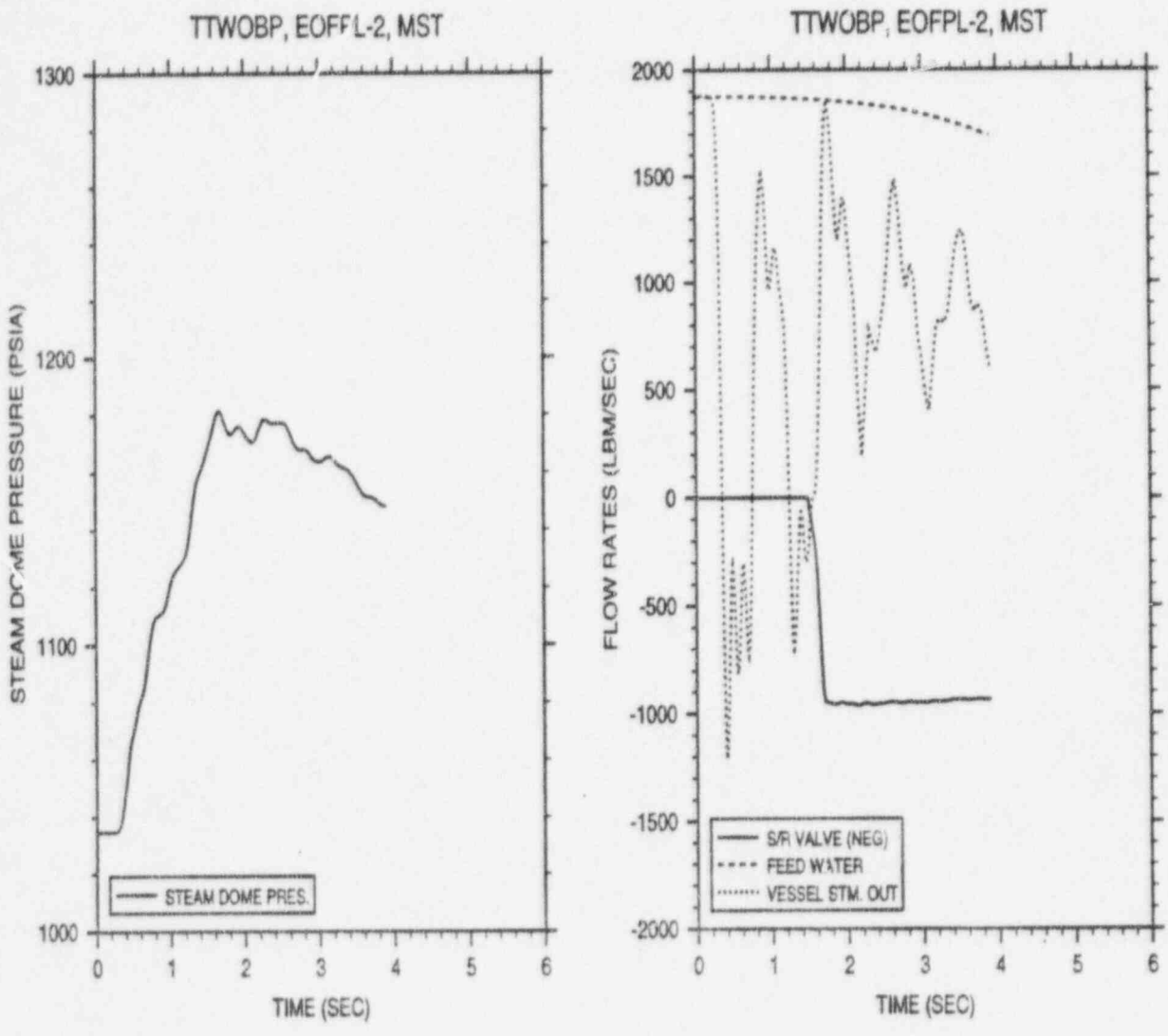

FIGURE 7.2.4
(Continued)

TURBINE TRIP WITHOUT BYPASS, EOFPL19-2000 MWD/ST
TRANSIENT RESPONSE VERSUS TIME, "MEASURED" SCRAM TIME

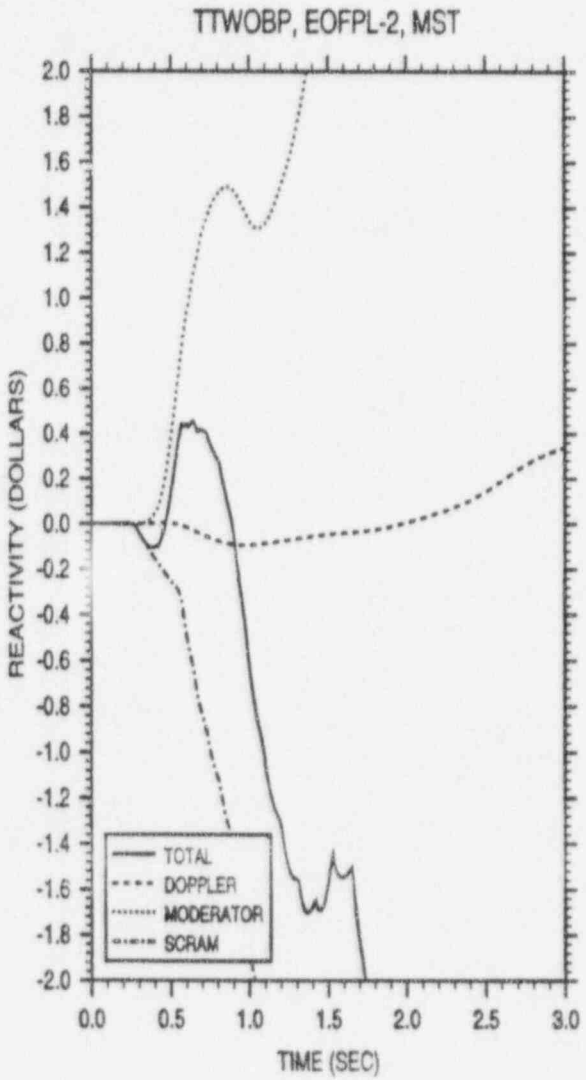

FIGURE 7.2.4
(Continued)

TURBINE TRIP WITHOUT BYPASS, EOFPL19-2000 MWD/ST
TRANSIENT RESPONSE VERSUS TIME, "MEASURED" SCRAM TIME

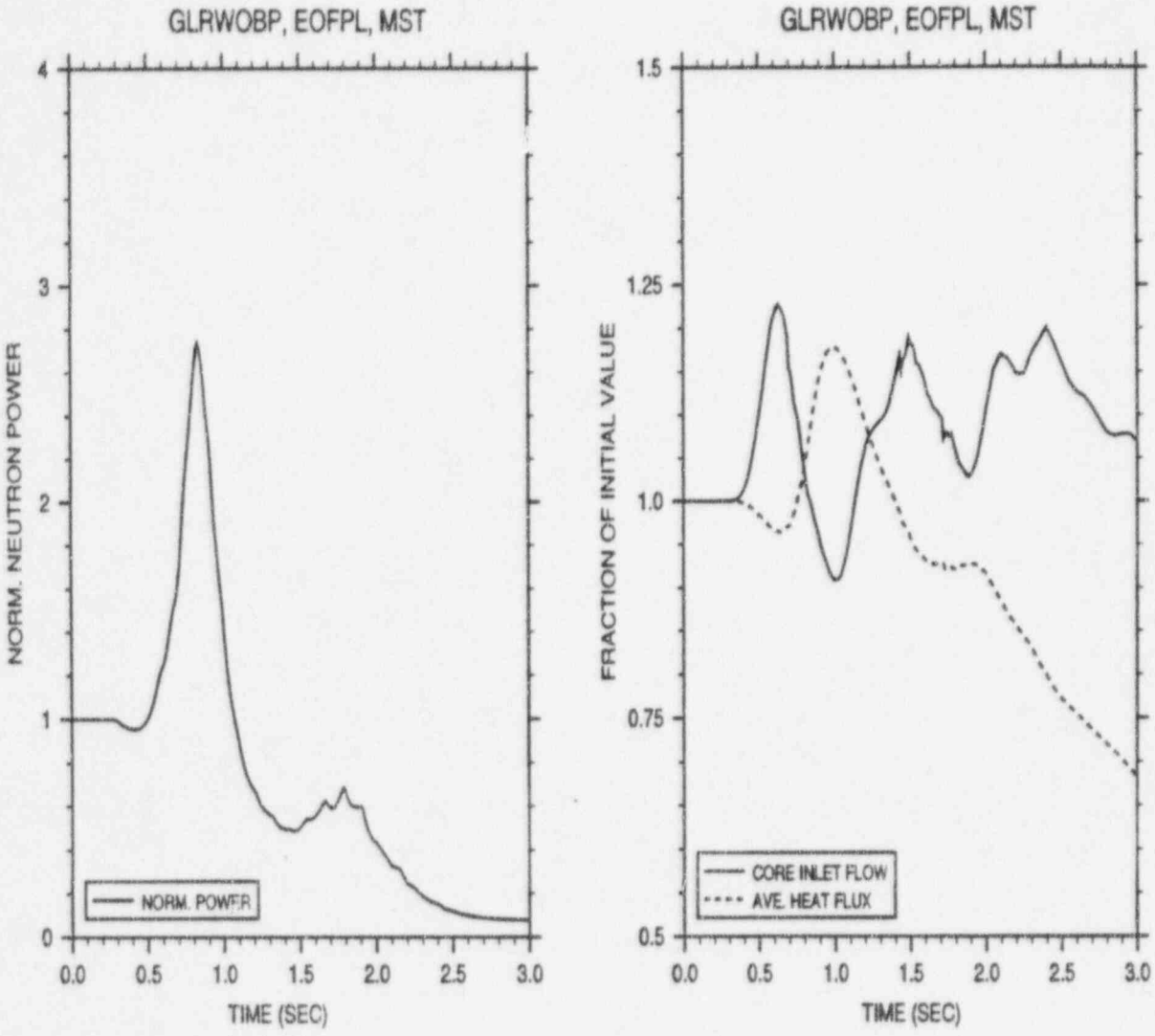

FIGURE 7.2.5

GENERATOR LOAD REJECTION WITHOUT BYPASS, EOFPL19
TRANSIENT RESPONSE VERSUS TIME, "MEASURED" SCRAM TIME

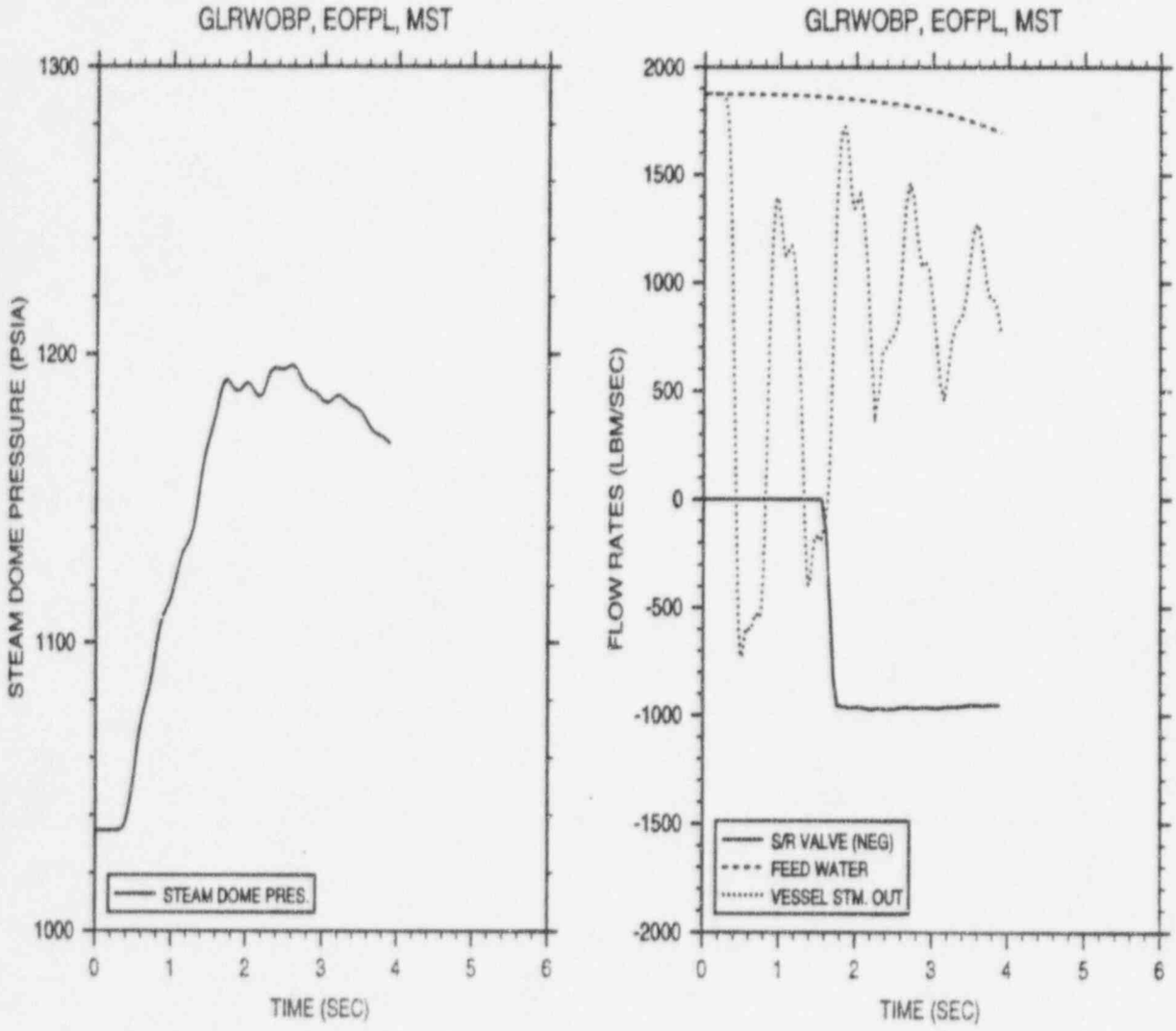

FIGURE 7.2.5
(Continued)

GENERATOR LOAD REJECTION WITHOUT BYPASS, EOFPL19
TRANSIENT RESPONSE VERSUS TIME, "MEASURED" SCRAM TIME

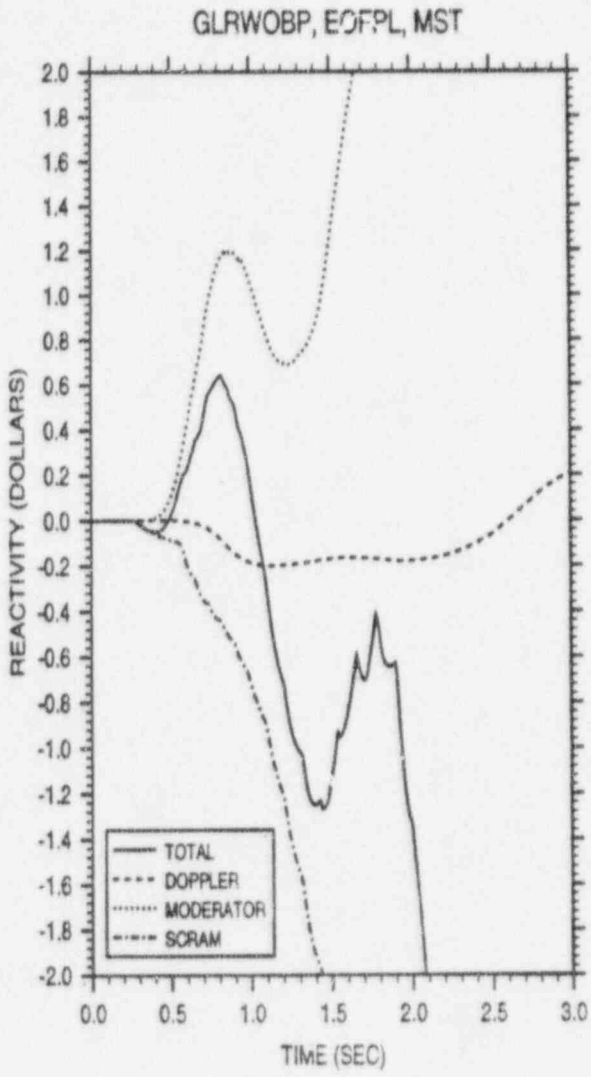

FIGURE 7.2.5
(Continued)

GENERATOR LOAD REJECTION WITHOUT BYPASS, EOFPL19
TRANSIENT RESPONSE VERSUS TIME, "MEASURED" SCRAM TIME

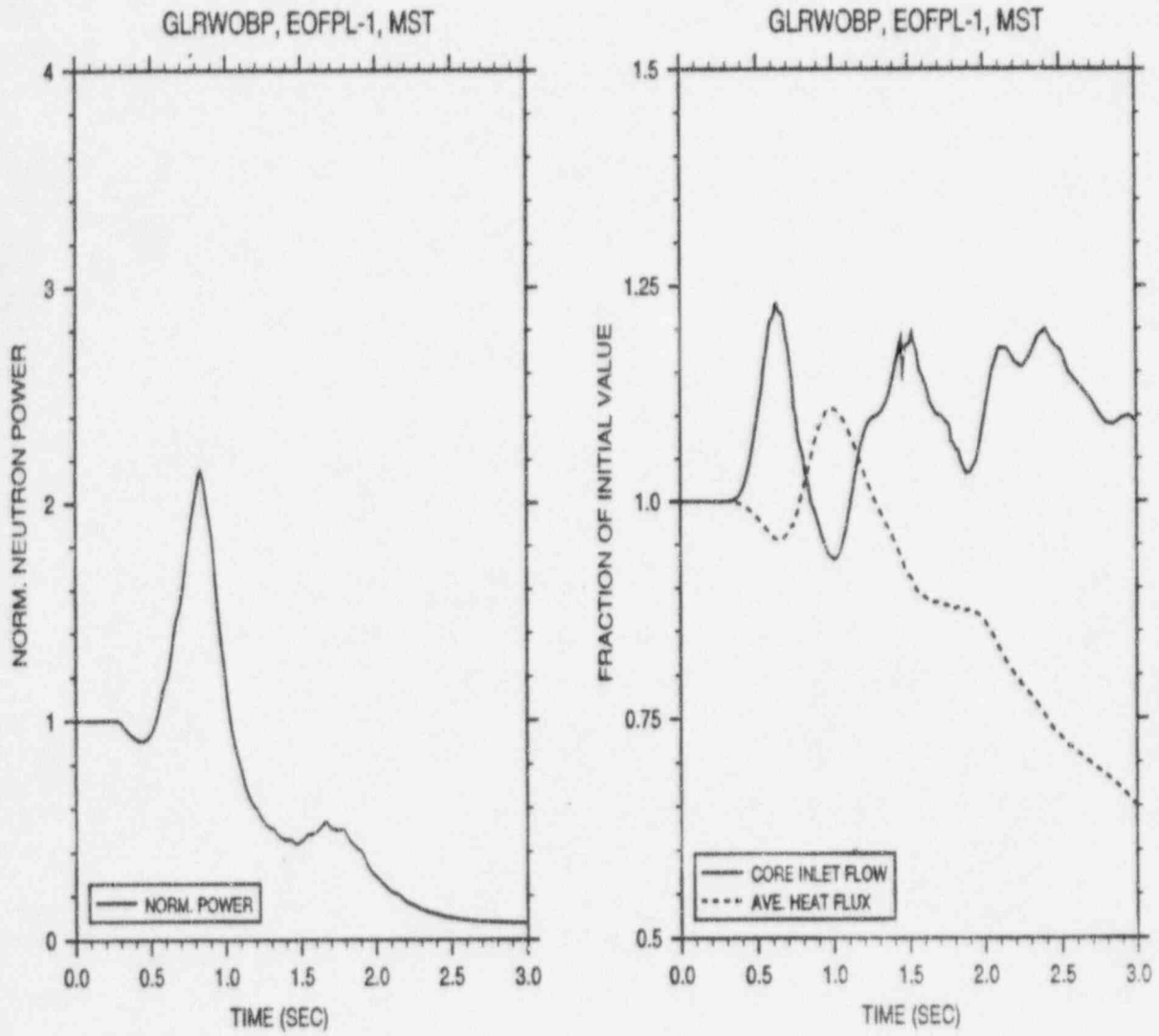

FIGURE 7.2.6

GENERATOR LOAD REJECTION WITHOUT BYPASS, EOFPL19-1000 MWD/ST
TRANSIENT RESPONSE VERSUS TIME, "MEASURED" SCRAM TIME

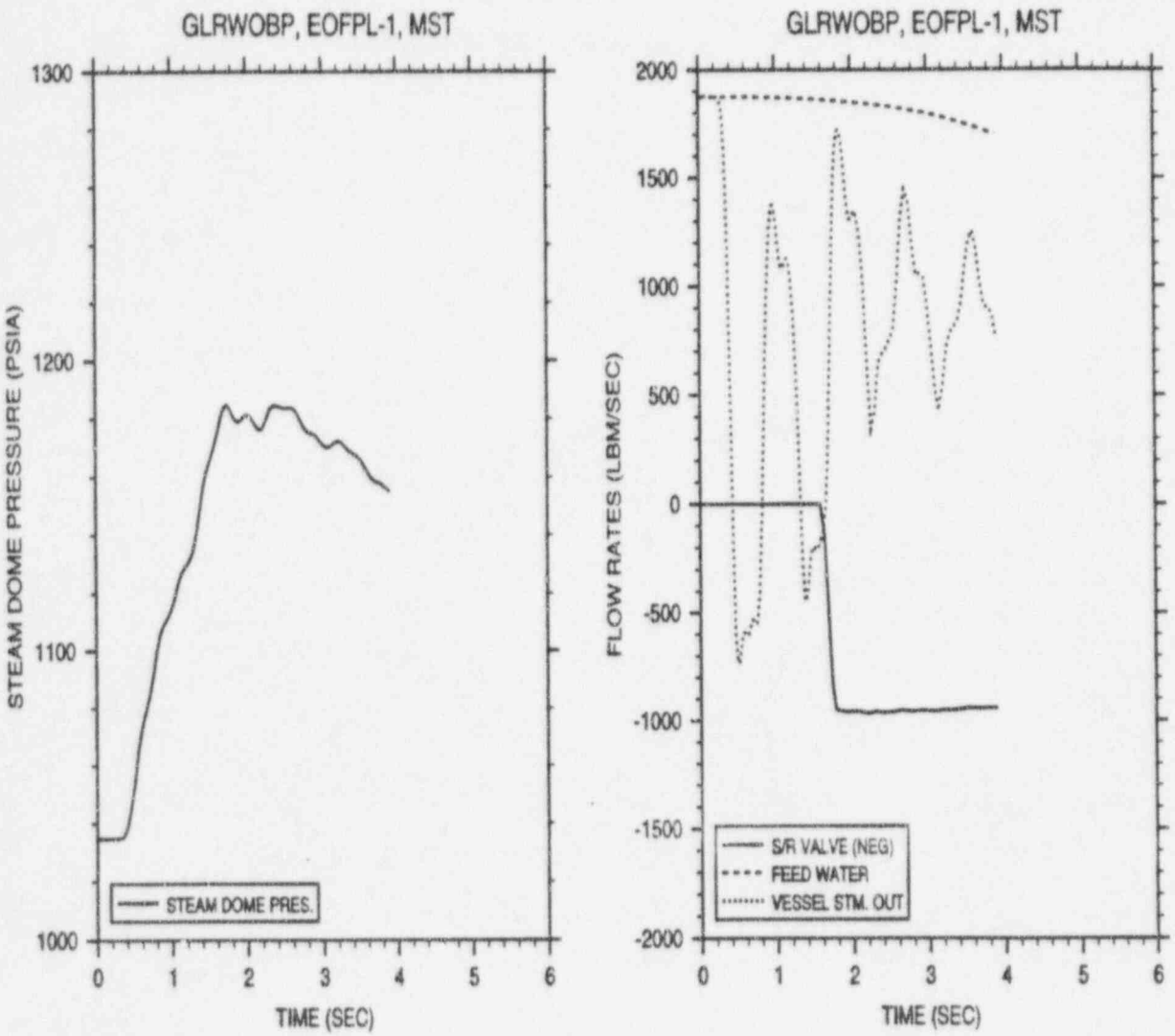

FIGURE 7.2.6
(Continued)

GENERATOR LOAD REJECTION WITHOUT BYPASS, EOFPL19-1000 MWD/ST
TRANSIENT RESPONSE VERSUS TIME, "MEASURED" SCRAM TIME

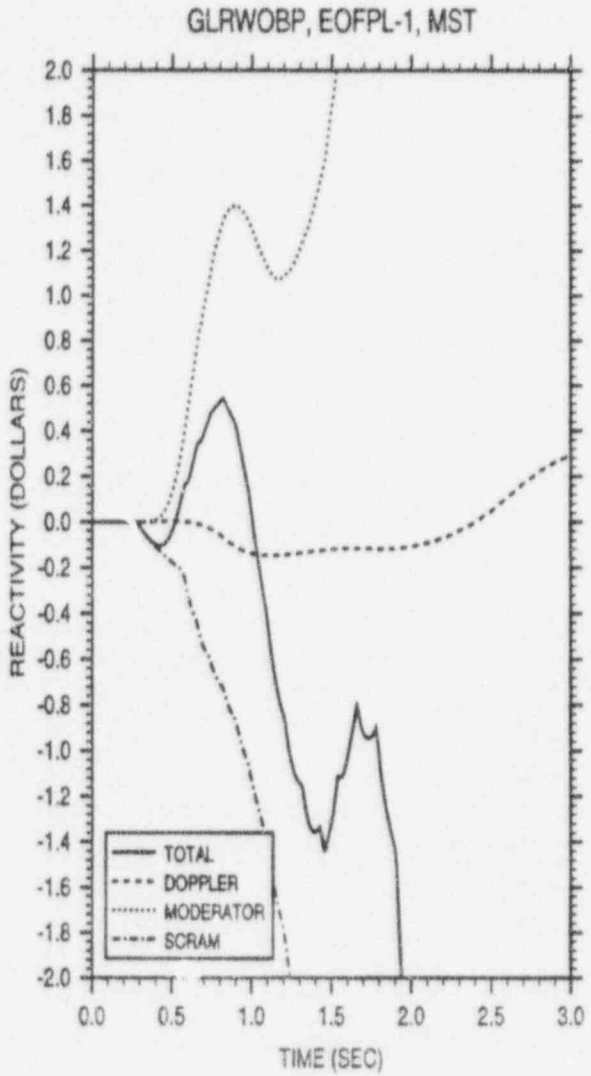

FIGURE 7.2.6
(Continued)

GENERATOR LOAD REJECTION WITHOUT BYPASS, EOFPL19-1000 MWD/ST
TRANSIENT RESPONSE VERSUS TIME, "MEASURED" SCRAM TIME

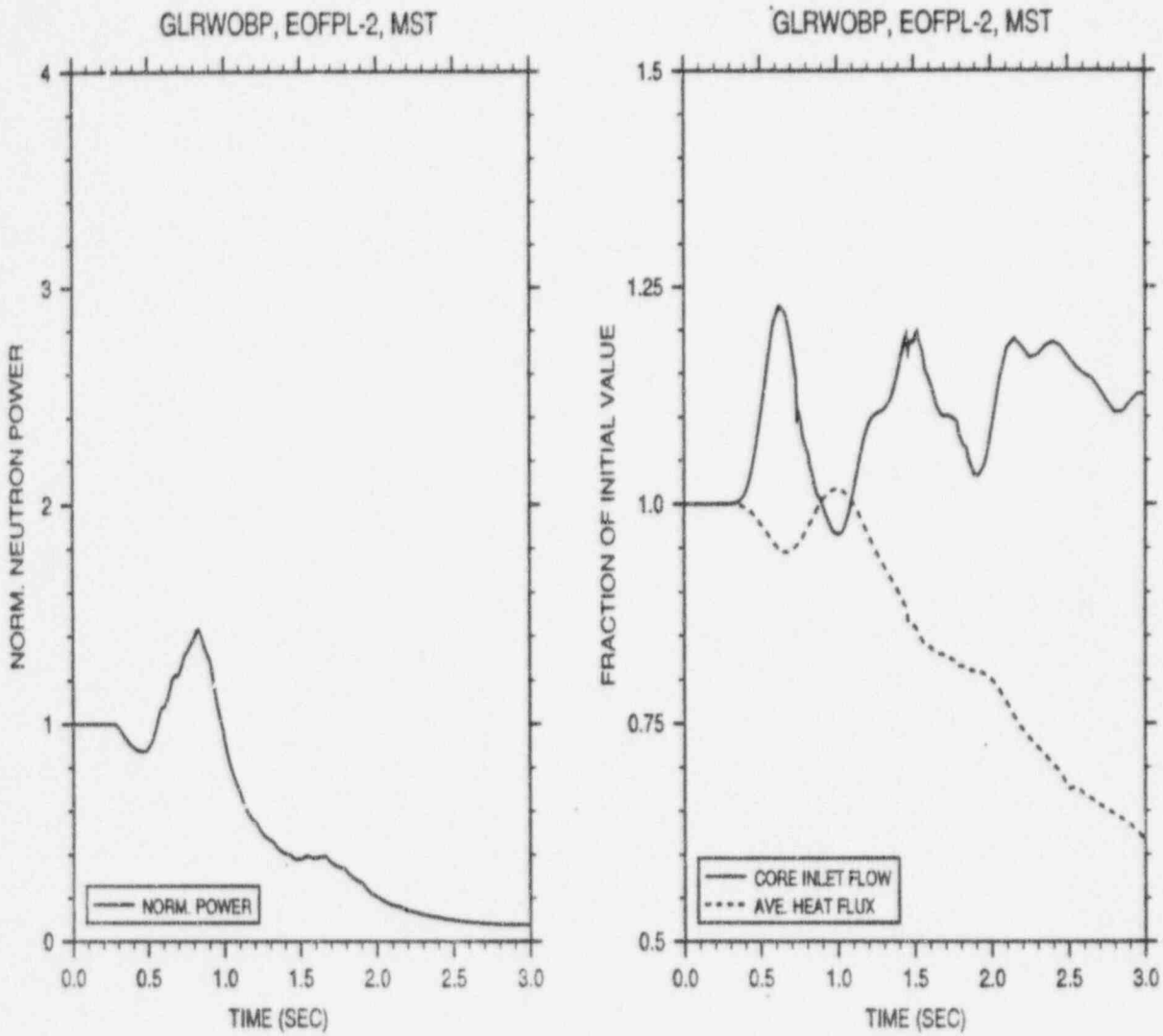

FIGURE 7.2.7

GENERATOR LOAD REJECTION WITHOUT BYPASS, EOFPL19-2000 MWD/ST
TRANSIENT RESPONSE VERSUS TIME, "MEASURED" SCRAM TIME

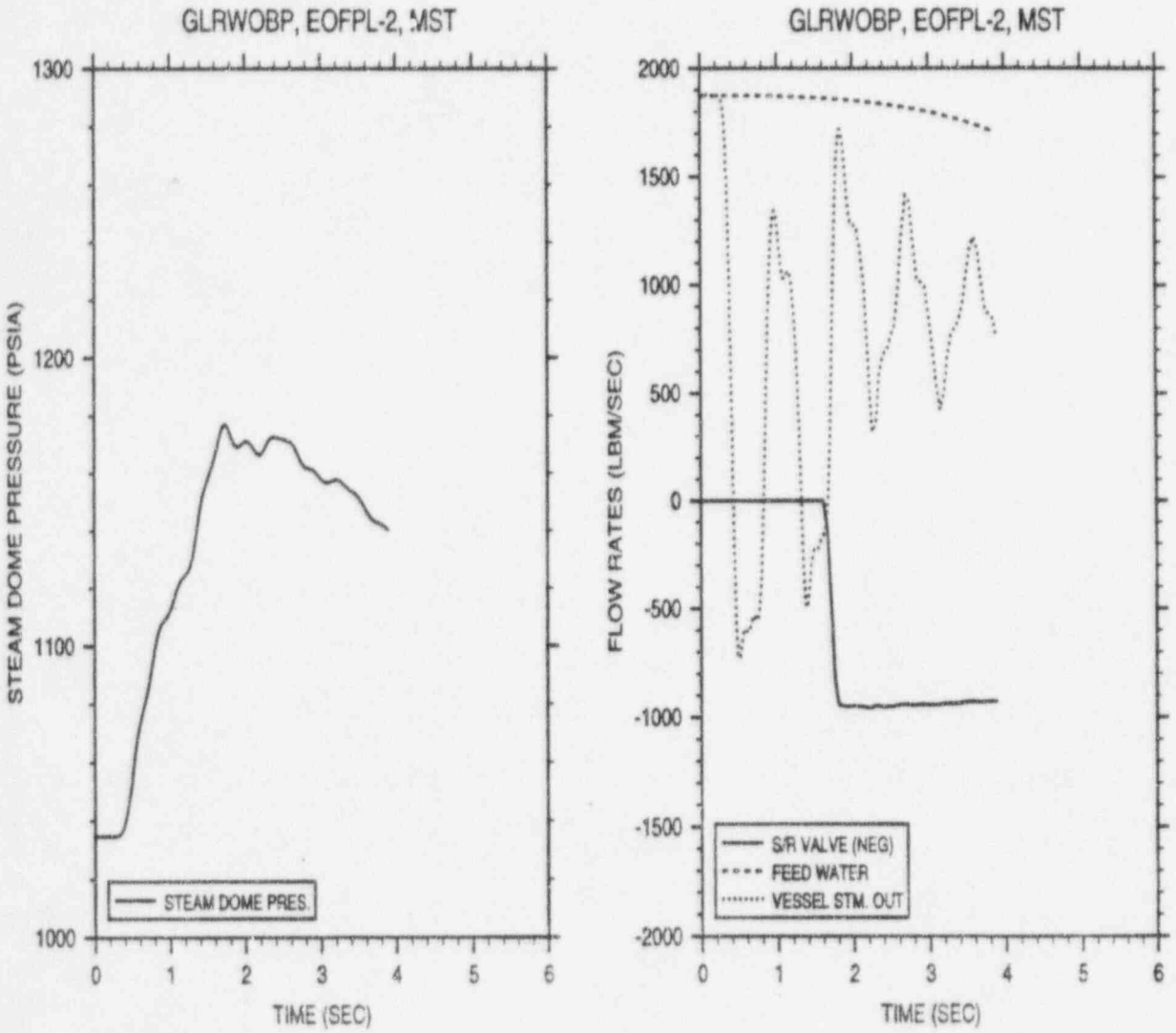

FIGURE 7.2.7
(Continued)

GENERATOR LOAD REJECTION WITHOUT BYPASS, EOFPL19-2000 MWD/ST
TRANSIENT RESPONSE VERSUS TIME, "MEASURED" SCRAM TIME

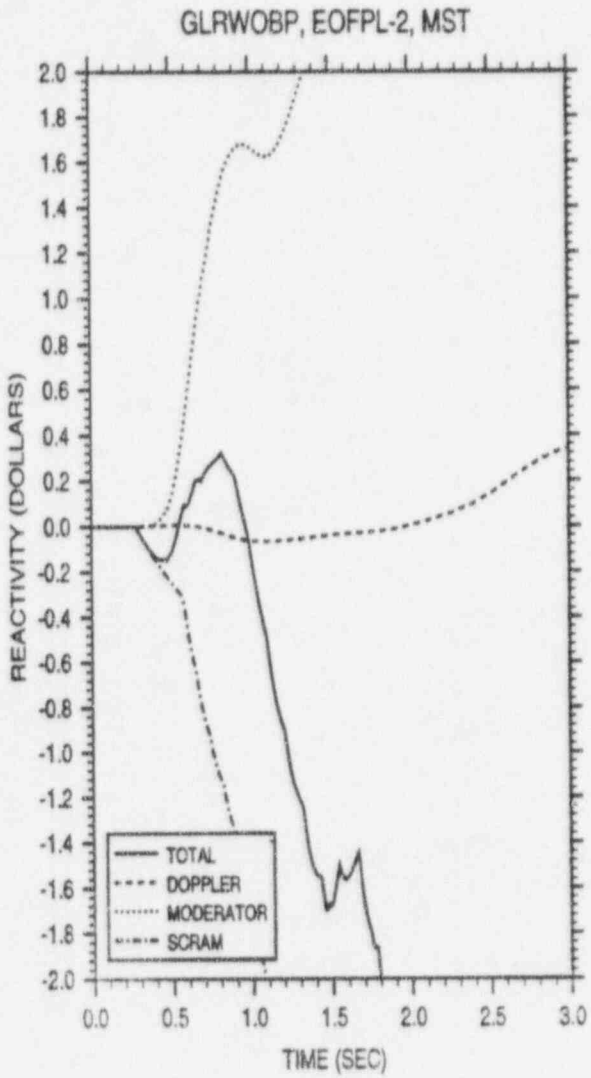

FIGURE 7.2.7
(Continued)

GENERATOR LOAD REJECTION WITHOUT BYPASS, EOFPL19-2000 MWD/ST
TRANSIENT RESPONSE VERSUS TIME, "MEASURED" SCRAM TIME

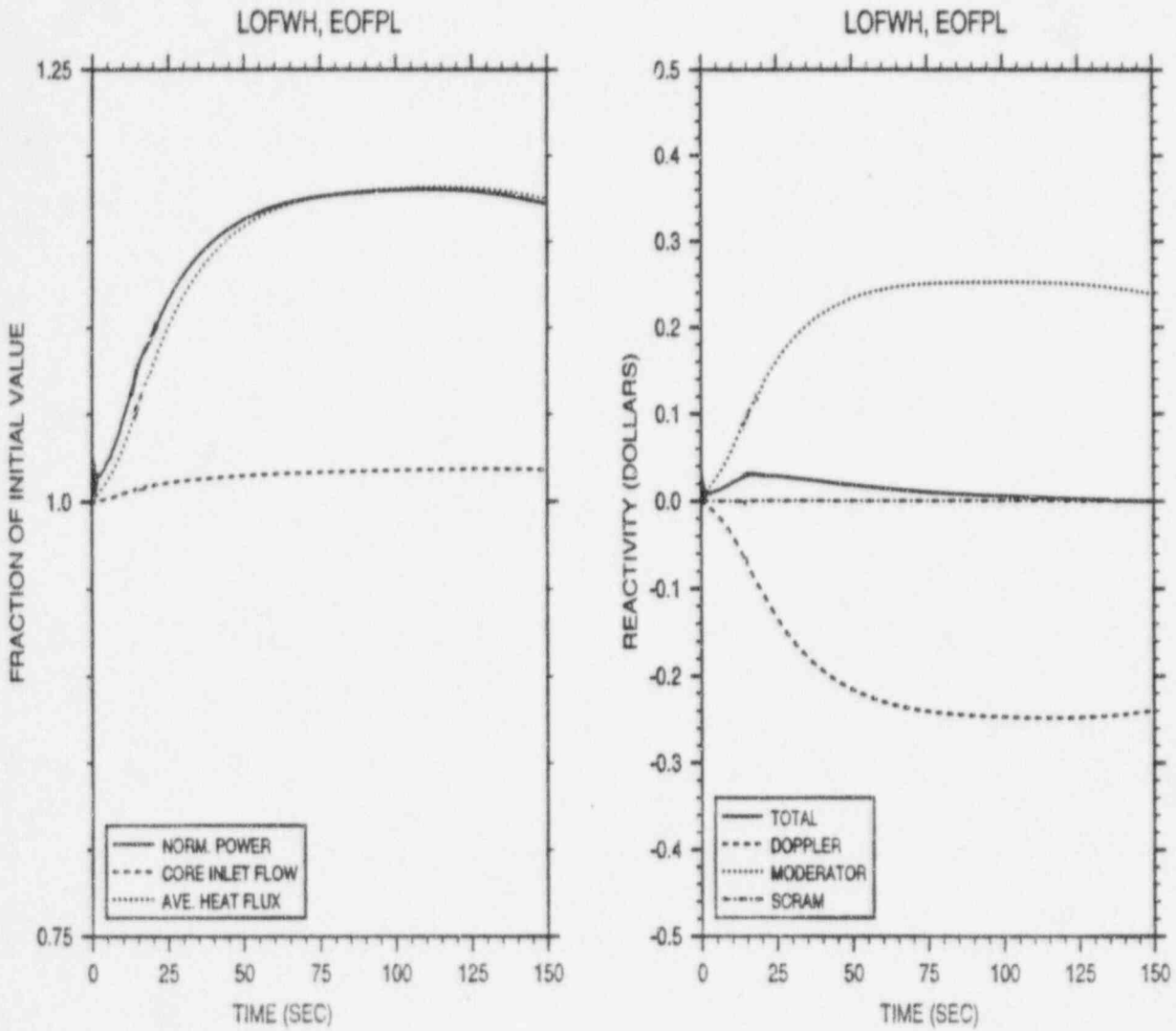

FIGURE 7.3.1

LOSS OF 100°F FEEDWATER HEATER (LIMITING CASE)
TRANSIENT RESPONSE VERSUS TIME

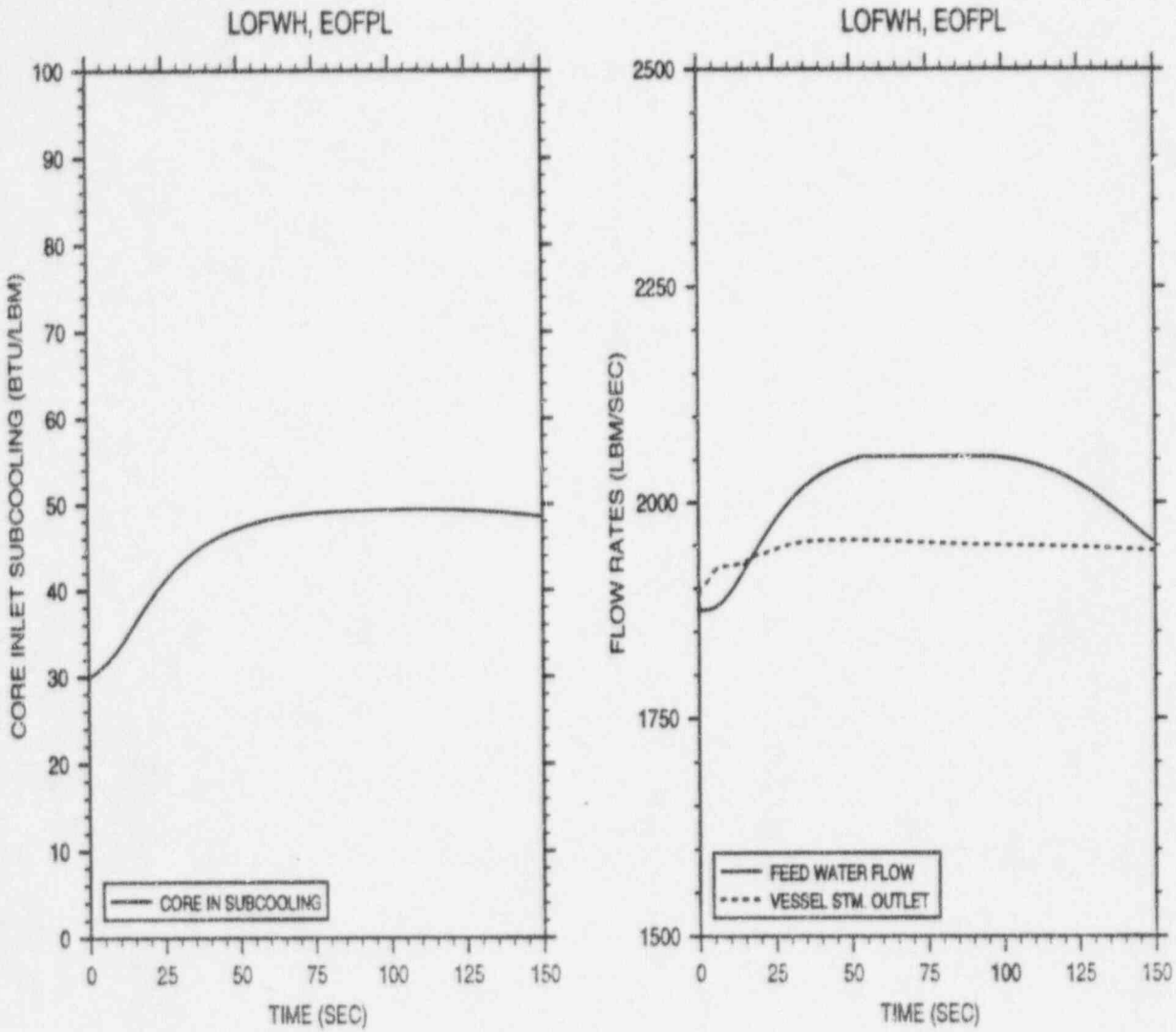

FIGURE 7.3.1
(Continued)

LOSS OF 100°F FEEDWATER HEATER (LIMITING CASE)
TRANSIENT RESPONSE VERSUS TIME

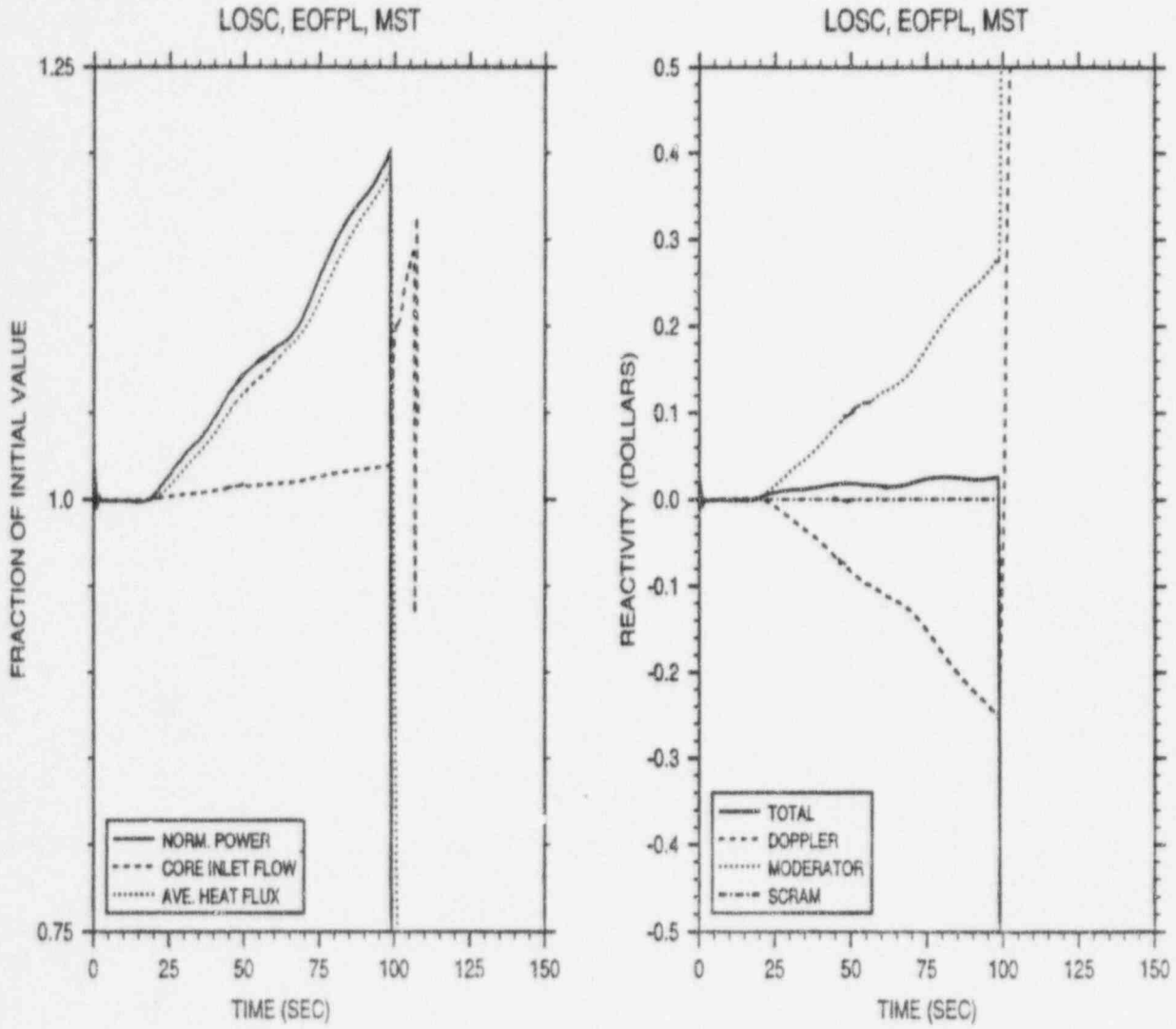

FIGURE 7.3.2

LOSS OF STATOR COOLING TRANSIENT RESPONSE VERSUS TIME

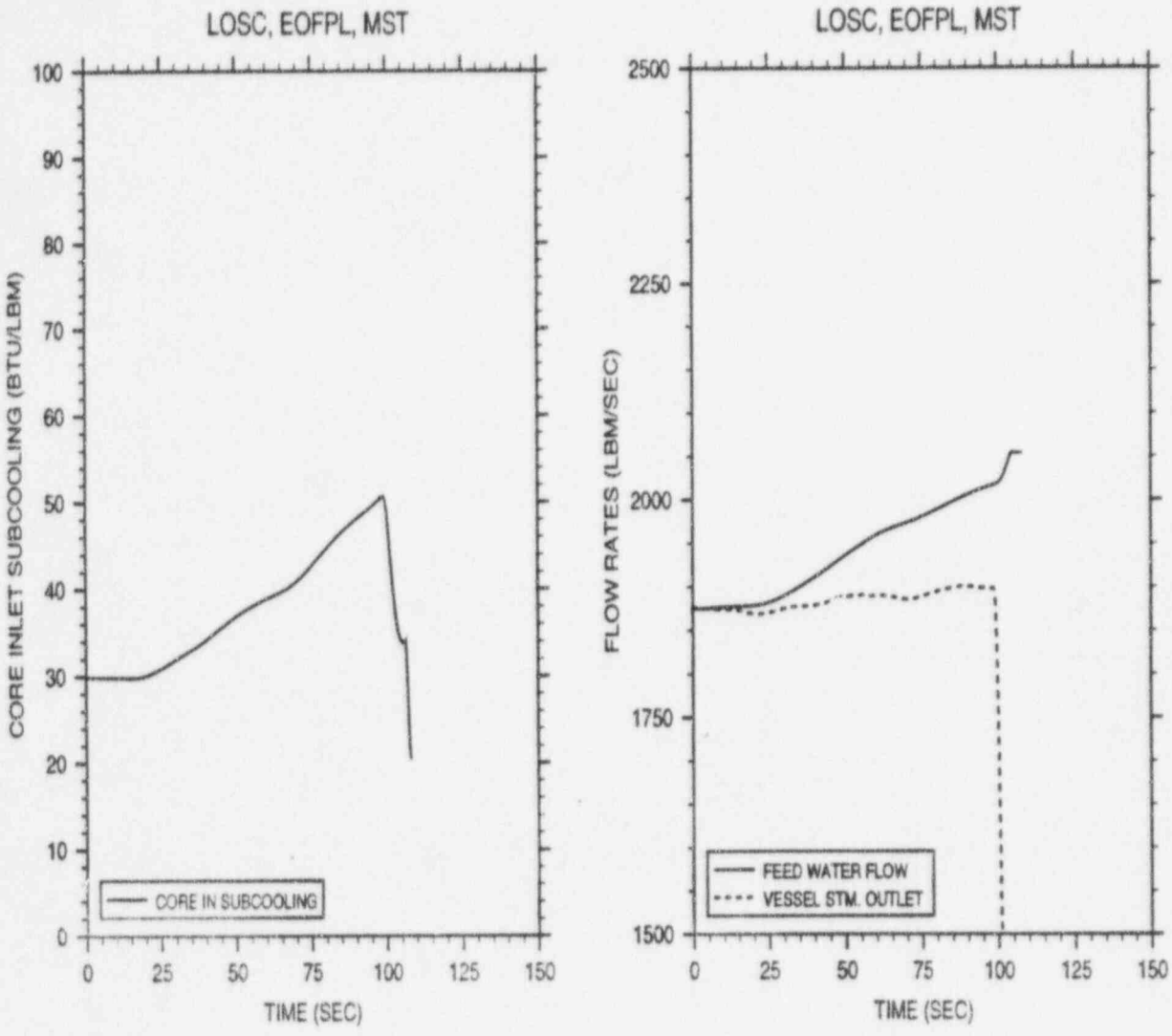

FIGURE 7.3.2
(Continued)

LOSS OF STATOR COOLING TRANSIENT RESPONSE VERSUS TIME

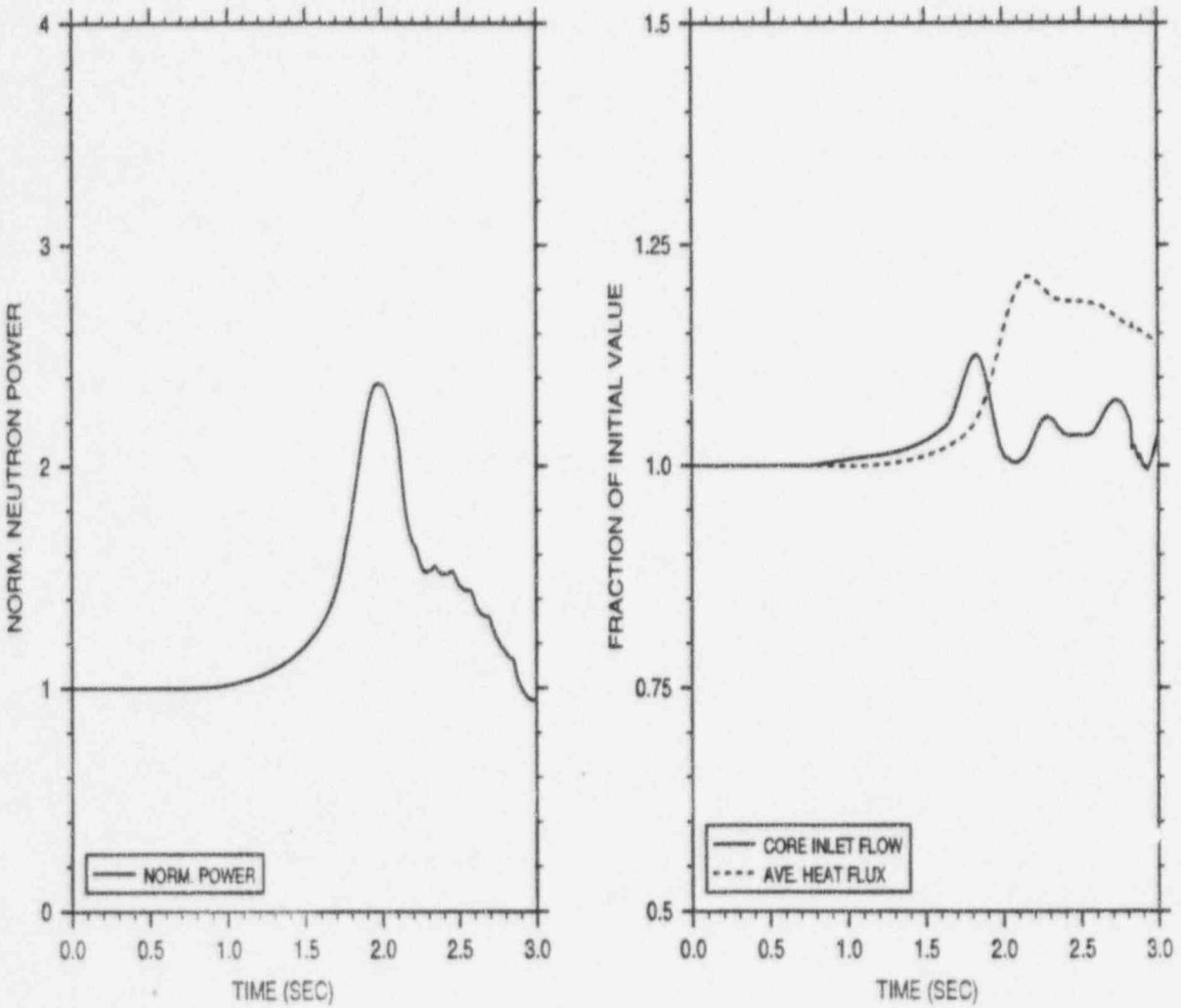

FIGURE 7.4.1

MSIV CLOSURE, FLUX SCRAM, EOFPL19
TRANSIENT RESPONSE VERSUS TIME, "67B" SCRAM TIME

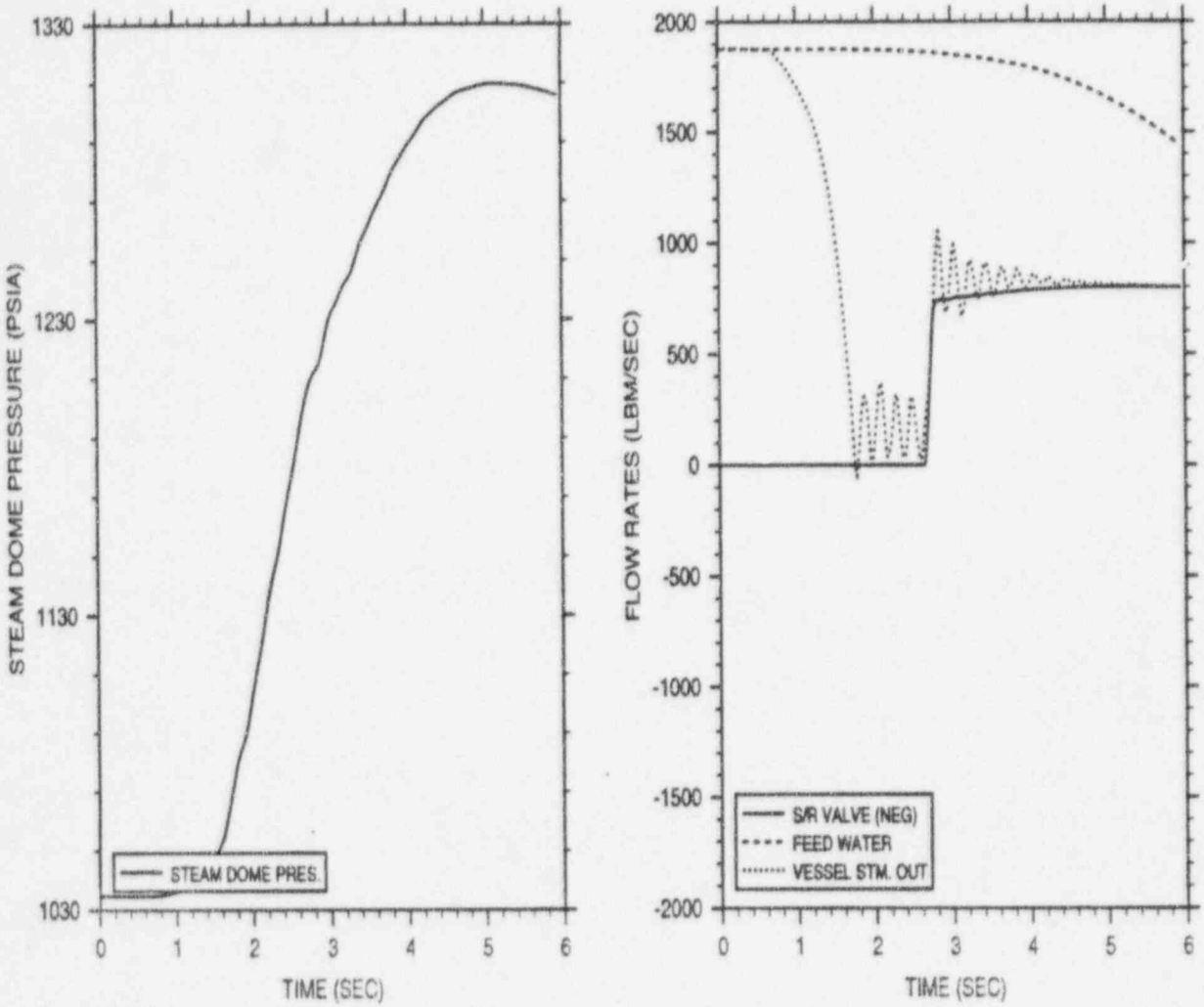

FIGURE 7.4.1
(Continued)

MSIV CLOSURE, FLUX SCRAM, EOFPL19
TRANSIENT RESPONSE VERSUS TIME, "67B" SCRAM TIME

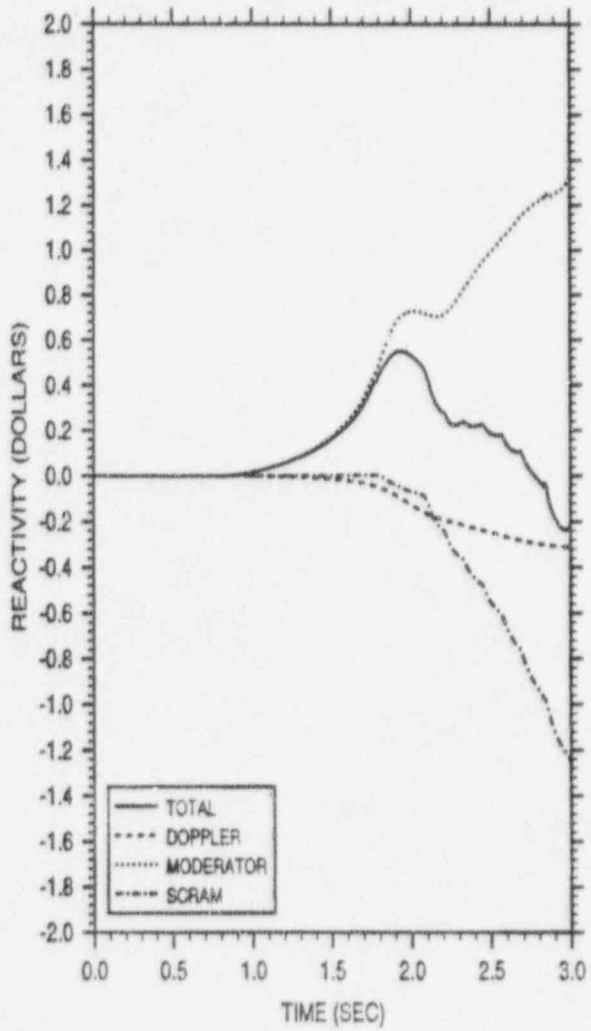

FIGURE 7.4.1
(Continued)

MSIV CLOSURE, FLUX SCRAM, EOFPL19
TRANSIENT RESPONSE VERSUS TIME, "67B" SCRAM TIME

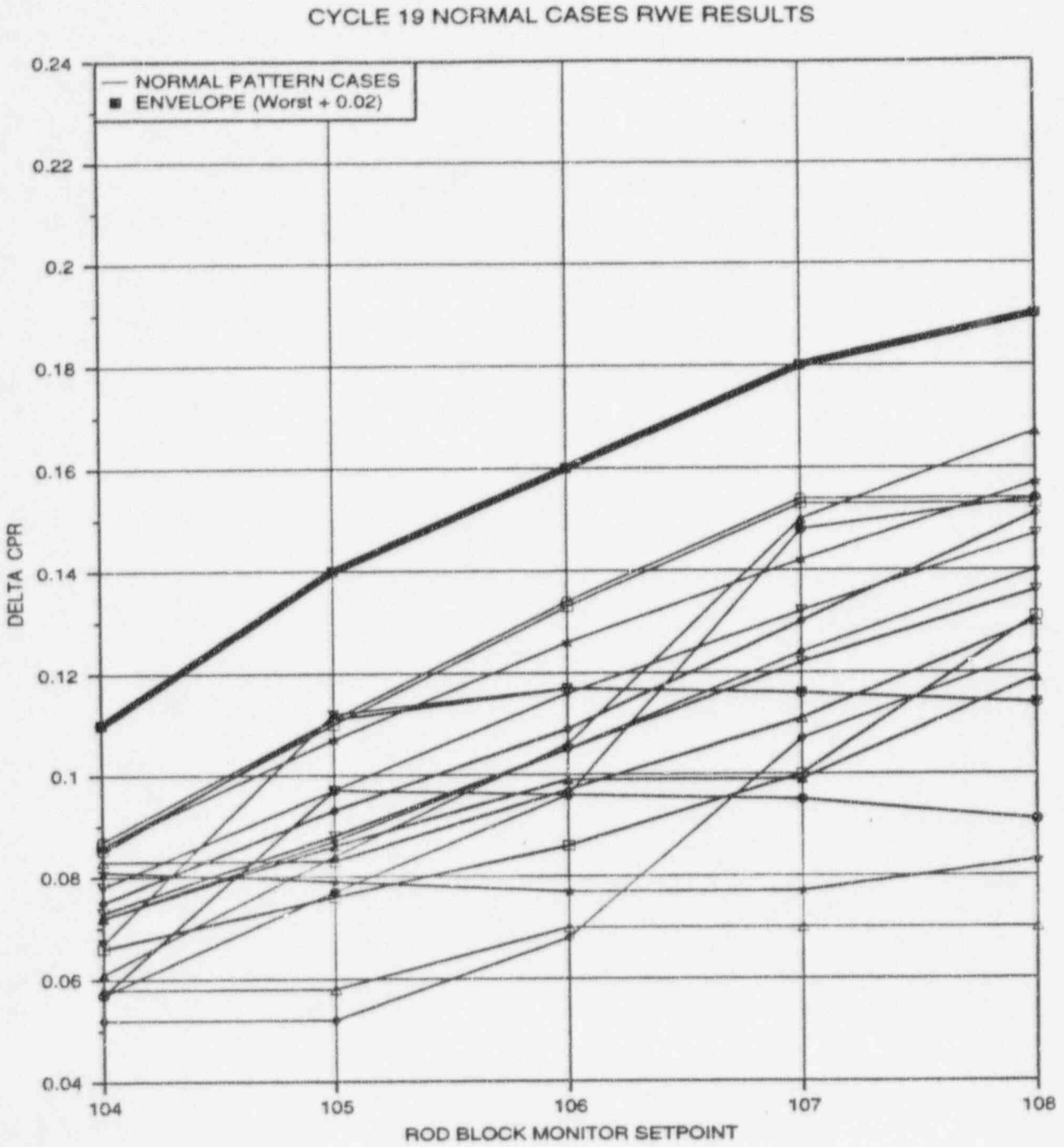

FIGURE 7.5.1

VY CYCLE 19 NORMAL RWE CASES RESULTS
- ΔCPR VERSUS RBM SETPOINT

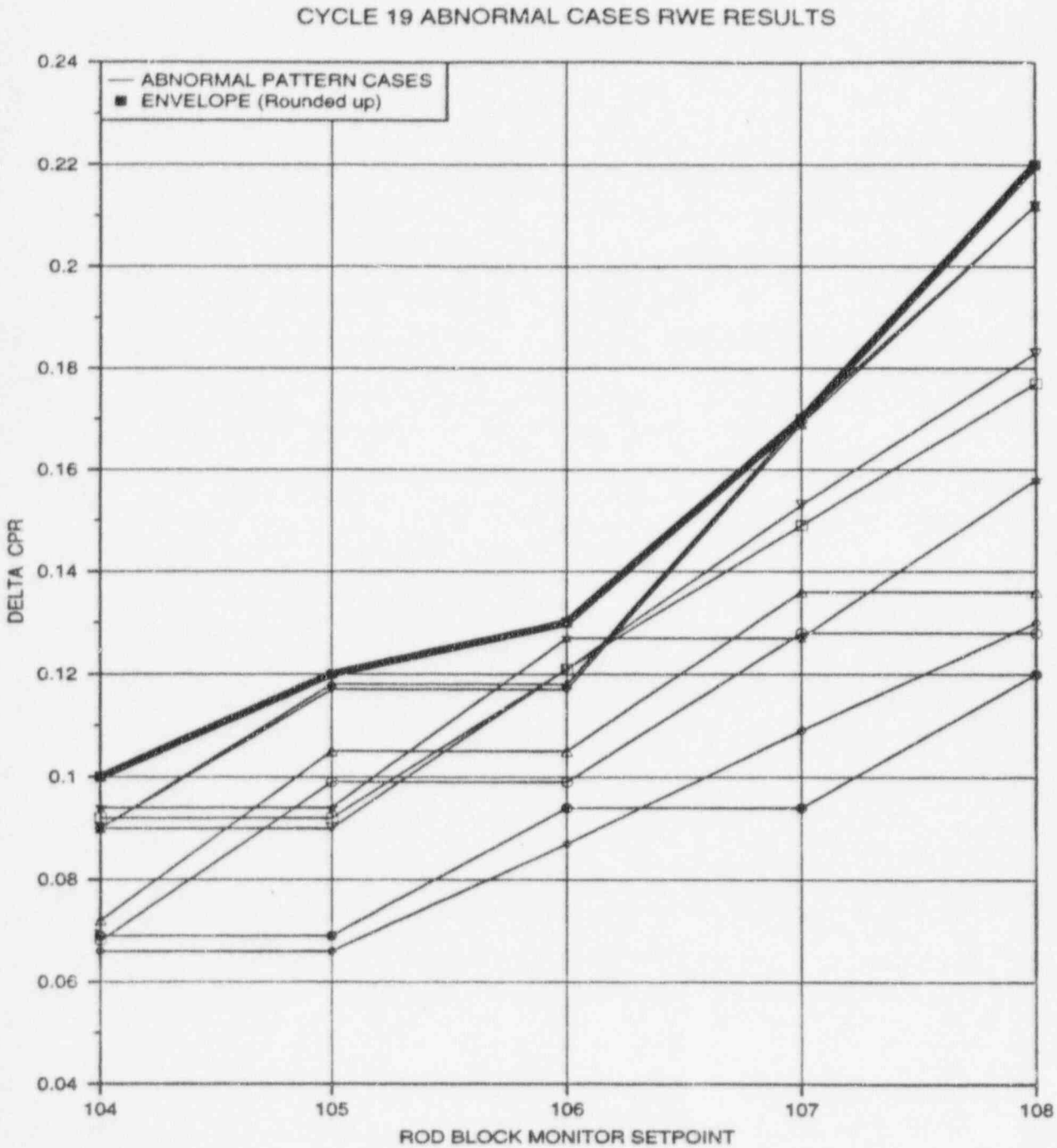

FIGURE 7.5.2

VY CYCLE 19 ABNORMAL RWE CASES RESULTS
- ΔCPR VERSUS RBM SETPOINT

8.0 DESIGN BASIS ACCIDENT ANALYSIS

8.1 Control Rod Drop Accident Results

The control rod sequences are a series of rod withdrawal and banked withdrawal instructions specifically designed to minimize the worths of individual control rods. The sequences are examined so that, in the event of the uncoupling and subsequent free fall of the rod, the incremental rod worth is acceptable. Incremental rod worth refers to the fact that rods beyond Group 2 are banked out of the core and can only fall the increment from full-in to the rod drive withdrawal position. Acceptable worth is one which produces a maximum fuel enthalpy less than 280 calories per gram.

Some out-of-sequence control rods could accrue potentially high worths. However, the Rod Worth Minimizer (RWM) will prevent withdrawing an out-of-sequence rod, if accidentally selected. The RWM is functionally tested before each startup.

The sequence in the RWM will take the plant from All Rods In (ARI) to well above 20% core thermal power. Above 20% power even multiple operator errors will not create a potential rod drop situation above 280 calories per gram[29],[30],[31]. Below 20% power, however, the sequences must be examined for incremental rod worth. This is done throughout the cycle using the full core, xenon-free SIMULATE-3 model.

Both the A and B sequences were examined at various exposures throughout the cycle. For startup, the rods are grouped, as shown in Figures 8.1.1 and 8.1.2, and are pulled in numerical order. All the rods in one group are pulled out before the pulling of the next group begins. The rods in the first two groups are individually pulled from full-in to full-out. Beyond Group 2, the rods are banked out using procedures which reduce the rod incremental worths[32],[33].

The potentially high worths that occur in pulling the rods in Group 1 are ignored because the reactor is subcritical in Group 1. Therefore, if a rod drops from any configuration in the first group, its excess reactivity contribution to the Rod Drop Accident (RDA) is zero. Successive reloads of axially zoned fuel have extended this subcriticality situation to the second group as well.

The second group of rods was examined using the following analysis method[34]. Both the A and B sequences were examined. It was found that the highest worth rod was the first rod in the second group. Any of the first four rod arrays, shown in Figures 8.1.1 and 8.1.2, may be designated as the first group pulled. However, a specific second group must follow as Table 8.1.1 illustrates. For added conservatism, each of the high worth rods in the second group were checked; i.e., one at a time, they were assigned to be the first rod pulled. This assures that in any sequence the actual worths will always be less than those calculated here.

Only that portion of the control rod worth above the SIMULATE-3 cold critical eigenvalue contributes to the rod drop accident. For conservatism, "critical" was defined as the SIMULATE-3 average cold critical K_{eff} minus 1% ΔK (reactivity anomaly criteria). The results of the Group 2 calculations, as presented in Table 8.1.2, fit under the bounding analysis of References 29 through 31.

Beyond Group 2, the rods are banked out of the core. This generally limits the incremental worth of a single rod drop; however, virtually all of the pre-drop cases in Group 3 are critical. Therefore, the entire dropped rod worth contributes toward the RDA excess reactivity insertion. The method used to evaluate Group 3 involved pulling Groups 1 and 2 out and banking Group 3 to varying positions. The types of cases examined included:

1. Banked positions 04, 08, 12, and 48 (full-out).

2. Group 3 rods pulled out of sequence, creating high flux regions.

3. Xenon-free conditions, both cold moderator and "standby" (i.e., 1020 psia).

4. Group 3 rods dropping from 00 (full-in) to the appropriate banked position.

5. Stuck rods from previously pulled Group 1 or 2 dropping from 00 to 48.

The highest worth results from the Group 3 analysis fit under the Group 2 results, presented in Table 8.1.2.

8.2 Loss-of-Coolant Accident Analysis

The LOCA analysis, performed in accordance with 10CFR50 Appendix K and the Safety Evaluation Reports[35],[36], demonstrates that Vermont Yankee, operating within the assumed conditions, complies with the LOCA limits specified in 10CFR50.46.

The LOCA analysis for the Reload Cycle is a combination of cycle specific analysis and a base analysis for Cycle 17[37]. Both analyses use the NRC-approved codes, FROSSTEY-2[9] and RELAP5YA[38]. The base analysis provided the break spectrum and the single failure conditions. The Reload Cycle analysis provided the verification that the base analysis was valid for the Reload Cycle changes.

Several changes have been made to the model during Cycle 18 since the Cycle 18 Core Performance Analysis Report[39]: 1) an error in the fuel behavior model in RELAP5YA was corrected, 2) the recirculation bypass valves were added as being open, 3) the LPCI flow was reduced by 500 gpm to account for the RHR minimum flow valve being open at all times except during shutdown cooling, and 4) a change in the trip logic for ECCS pressure permissive and ADS actuation to represent the containment under harsh environmental conditions. The model changes for Cycle 19 were: 1) the core spray flow was reduced by 300 gpm to allow the core spray minimum flow bypass valves to be open at all times and 2) minor cycle-specific changes to the physics data, stored energy and the central average region. All other assumed initial conditions and assumptions are the same for both analyses. Table 8.2.1 lists some of the key input assumptions but Reference 37 provides a more detailed listing of the input assumptions.

The Cycle 17 base analysis was performed for a combination of break size, break location, and single failure conditions. The break sizes range from 0.05 ft^2 to 7.28 ft^2. Five break locations were analyzed: main steam line, core spray line, feedwater line, recirculation loop suction and recirculation loop discharge. Five possible single failures were evaluated: low pressure coolant injection valve, high pressure coolant injection, DC power supply, diesel generator and one automatic depressurization system valve. The impact of the Gd_2O_3 on initial volume average temperature and material properties was included

Table 8.2.2 lists the individual PCT results for each of the changes identified above. The Reload Cycle analysis was performed for the limiting break size and two single failure conditions. The Reload Cycle analysis results show that the limiting break is 0.6 ft^2 in the recirculation loop at the pump discharge with one DC power supply as the single failure and loss of offsite power coincident with the break opening. The maximum PCT results was 1801.7°F. The Reload Cycle analysis also showed that the break spectrum performed for the base analysis remains valid for the Reload Cycle. The analysis shows compliance with the other 10CFR 50.46 limits: the calculated peak clad temperatures are well below the 2200°F limit, total cladding oxidation at the peak location is less than 17%; hydrogen generated in the core is less than 1%; and the core retains a coolable geometry with no clad rupture.

During the cycle, Vermont Yankee can adjust the core flow to account for reactivity changes rather than using the control rods. During this type of operation, core flow may be as low as 87% while at 100% power. To ensure the safety analysis bounds these conditions, the LOCA analysis was analyzed at 1698 MW_{th} power and 87% flow. The results showed that the 100% flow case bounded the low flow case.

The analysis showed that the MAPLHGR limits are not limited by a LOCA. Therefore, the MAPLHGR limits are set based on the thermal-mechanical analysis of the bundle. They are provided in Appendix A for all the fuel types in the Reload Cycle, as a function of average planar exposure. The analysis also verified that the single loop MAPLHGR multiplier, 0.83, is valid for the Reload Cycle.

8.3 Refueling Accident Results

If any assembly is damaged during refueling, then a fraction of the fission product inventory could be released to the environment. The source term for the refueling accident is the maximum gap activity within any bundle. The source term includes contributions from both noble gases and iodines. The calculation of maximum gap activity is based on the MAPLHGR operating limits, the maximum operating fuel centerline temperatures, and maximum bundle burnup. The fuel rod gap activity, internal pressure and centerline temperature for the Reload Cycle are bounded by the values used in Section 14.9 of the FSAR[40].

TABLE 8.1.1

CONTROL ROD DROP ANALYSIS - ROD ARRAY PULL ORDER

The order in which rod arrays are pulled is specific once the choice of the first group is made.

First Group Pulled Is:	Second Group Pulled Must Be:	Successive Group Is Banked Out
Array 1	Array 2	Arrays 3 or 4
Array 2	Array 1	Arrays 3 or 4
Array 3	Array 4	Arrays 1 or 2
Array 4	Array 3	Arrays 1 or 2

TABLE 8.1.2

VY CYCLE 19 CONTROL ROD DROP ANALYSIS RESULTS

Maximum Incremental Rod Worth Calculated Cold, Xenon-Free	0.94% ΔK
Bounding Analysis Worth for Enthalpy Less than 280 Calories per Gram [29],[30],[31]	1.30% ΔK

TABLE 8.2.1

LOCA ANALYSIS ASSUMPTIONS

Core Thermal Power (MW_{th})	1698.3
Total Core Flow ($10^6 lb_m/hr$)	48.0
Reactor Vessel Pressure (psia)	1067.0
Recirculation Loop Flow ($10^6 lb_m/hr$) - Each Loop	12.3
Feedwater Flow ($10^6 lb_m/hr$)	6.93
Feedwater Temperature (°F)	377.0
Water Level Above Top of Enriched Fuel (in.)	130.0
Containment Drywell Pressure (psia)	16.5
Containment Wetwell Pressure (psia)	14.7
Containment Wetwell Liquid Temperature (°F)	165.0
Maximum Bundle Power (MW_{th})	7.3
Maximum Average Planar Linear Heat Generation Rate (kW/ft)	13.6*
Maximum Linear Heat Generation Rate (kW/ft)	14.4**

---

* Plus Calorimetric and TIP Reading Uncertainties (8.9%): 13.6 × 1.089 = 14.8 kW/ft

** Plus Calorimetric and TIP Reading Uncertainties (9.2%): 14.4 × 1.092 = 15.72 kW/ft

TABLE 8.2.2

LOCA ANALYSIS RESULTS, PEAK CLADDING TEMPERATURE

Descriptions of Model Change	PCT (°F)
Correct conservative error in the fuel behavior model in RELAP5YA*	1778.1
Accounting for the harsh environmental conditions	1780.5
Opening the Recirculation Bypass Valves	1764.5
LPCI flow reduction with the opening of the RHR Minimum Flow Valve	1793.9
Changing the fuel for Cycle 19 and LPCS flow reduction with the opening of the Core Spray Minimum Flow Bypass Valve and the above three changes	1801.7

* Already reported to the NRC in accordance with 10CFR50.46(a)(3)(ii).

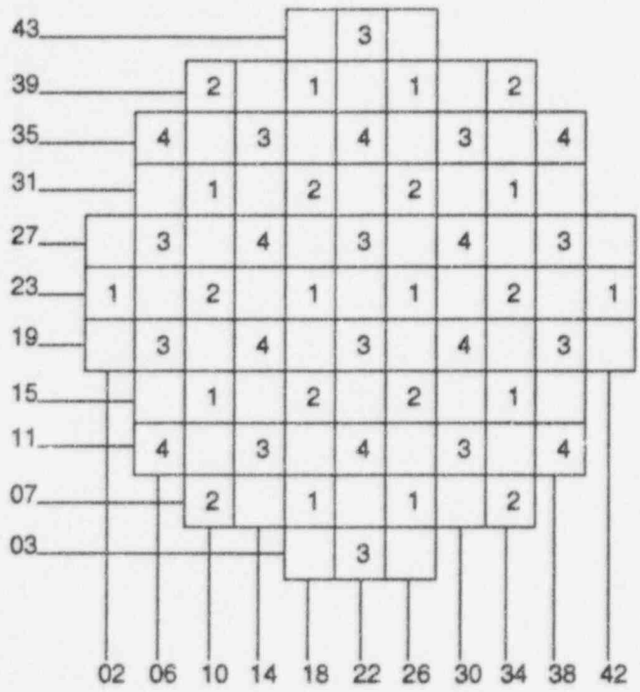

FIGURE 8.1.1

FIRST FOUR ROD ARRAYS PULLED IN THE A SEQUENCES

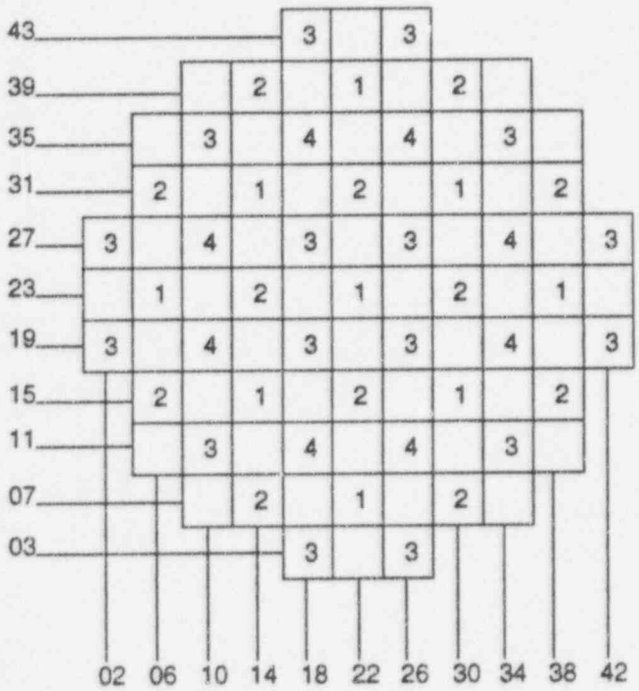

FIGURE 8.1.2

FIRST FOUR ROD ARRAYS PULLED IN THE B SEQUENCES

9.0 STABILITY ANALYSIS

The reload core design is analyzed each fuel cycle to assure that the potential occurrence of a thermal hydraulic oscillation or instability can be prevented through avoidance of operation in conditions susceptible to an instability. An assessment of the APRM flow biased scram setpoints is also made to assure that for the expected mode of oscillation in Vermont Yankee, the core wide mode, the setpoints are adequate to prevent exceeding the FCISL if an oscillation is not prevented and remains undetected by an operator. The identification of operating conditions susceptible to instabilities is conservatively predicted for the operating cycle through application of the BWROG stability exclusion region methodology [41] and with the LAPUR code [42]. The BWROG application involves probing high powered, low flow conditions for a decay ratio of 0.8, the upper limit for acceptable operation of the reactor at off nominal conditions. Several operating states from natural circulation to approximately 60% flow and power are calculated to form a boundary at a 0.8 decay ratio. Operation above this boundary or in the "exclusion region" is prohibited for normal operation. For Cycle 19, LAPUR was applied to evaluate the relative stability characteristics of the reload core to confirm that the exclusion boundary calculated with the BWROG methodology remains valid.

Results of the analysis for the Cycle 19 exclusion region are shown in Figure A.1, with the corresponding data points composing the boundary contained in Table A.5. Also, contained in Figure A.1 is an additional boundary referred to as the buffer region. This region is an area of operation where, under unexpected operating circumstances, it may be possible to experience an instability. Operation within the buffer region requires the use of the plant process computer stability monitor. The stability monitor provides the decay ratio for the actual operating conditions. If while operating in the buffer region the monitor calculates a decay ratio of 0.8, the operator is directed to exit the buffer region. Should the stability monitor fail to function, the buffer region is considered part of the exclusion region.

Justification of the APRM flow biased scram for detecting and suppressing a core wide mode instability is carried out using the BWROG detect and suppress reload methodology [41],[43]. The purpose of the reload methodology is to confirm that the combination of APRM trip setpoints and operating MCPR limits provides a high confidence that the FCISL will not be violated for the anticipated core wide oscillations. It consists of checking the operating MCPR limits, the fuel type and that the hot bundle oscillation characteristics have not changed. For Cycle 19, the MCPR operating limits have been

The increase provides a more conservative initial operating state. The fuel type, GE9B, has not changed since the last analysis for Cycle 15 [44]. The hot bundle oscillation characteristics have also not changed since Cycle 15, nor have the flow biased scram setpoints, the two primary factors which would influence the hot bundle oscillation magnitude prior to power suppression by the APRM scram. Thus, it is concluded that the APRM flow biased scram setpoints remain adequate for oscillation suppression prior to exceeding the MCPR.

10.0 STARTUP PROGRAM

Following refueling and prior to vessel reassembly, fuel assembly position and orientation will be verified and videotaped by underwater television.

The Vermont Yankee Startup Program will include process computer data checks, shutdown margin demonstration, in-sequence critical measurement, rod scram tests, power distribution comparisons, TIP reproducibility, and TIP symmetry checks. The content of the Startup Test Report will be similar to that sent to the Office of Inspection and Enforcement in the past[45].

11.0 CONCLUSION

This report presented the design information, calculational results, and operating limits pertinent to the operation of the Reload Cycle. The core is designed to consist of 120 new GE-9B fuel bundles and 248 irradiated GE-9B fuel bundles. The shutdown margin for the Reload Cycle is greater than the Technical Specification limit. The bundles used in the Reload Cycle do not exceed the Technical Specification limit of 1.31 K_{∞} for storage in the spent fuel pool or the new fuel storage facility. The transient analysis has: 1) determined the MCPR operating limits so that the FCISL is not violated for the transients considered, 2) assured that the thermal and mechanical overpower limits are not exceeded during the transient, 3) demonstrated compliance with the ASME vessel code limits and 4) assured a pressure margin greater than 25 psi below the safety valve actuation settings. The control rod drop worth is less than the bounding analysis which demonstrates a maximum fuel enthalpy less than the Technical Specification limit of 280 calories per gram. The LOCA analysis demonstrates compliance with the acceptance criteria specified in 10CFR50.46. The fuel rod gap activity, internal pressure and centerline temperature are bounded by the values used in Section 14.9 of the FSAR which demonstrates the limits of 10CFR100 are not exceeded for a refueling accident. The stability analysis has defined an exclusion and buffer regions that assure the 10CFR50 Appendix A, General Design Criteria 10 and 12 are met for the Reload Cycle.

REFERENCES

1. R. C. Paulson, Vermont Yankee Cycle 17 Summary Report, YAEC-1919 (October 1995).

2. General Electric Company, General Electric Standard Application for Reactor Fuel (GESTARII), NEDE-24011-P-A-13, GE Company Proprietary, as amended (August 1996).

3. General Electric Company, General Electric Fuel Bundle Designs, NEDE-31152P, Revision 5, GE Company Proprietary, as amended (June 1996).

4. GE Letter, P. J. Savoia to R. T. Yee, "Transmittal of Documentation for Vermont Yankee Reload 18 Fuel Bundle," PJS95133 (August 29, 1995).

5. A. S. DiGiovine, J. P. Gorski, and M. A. Tremblay; SIMULATE-3 Validation and Verification; YAEC-1659-A (September 1988).

6. R. A. Woehlke, et al.; MICBURN-3/CASMO-3/TABLES-3/SIMULATE-3 Benchmarking of Vermont Yankee Cycles 9 through 13; YAEC-1683-A (March 1989).

7. B. Y. Hubbard, et al.; End-of-Full-Power-Life Sensitivity Study for the Revised BWR Licensing Methodology; YAEC-1822 (October 1991).

8. K. E. St.John, S. P. Schultz and R. P. Smith; Methods for the Analysis of Oxide Fuel Rod Steady-State Thermal Effects; YAEC-1912P-A (January 1995).

9. USNRC Letter to L. A. Tremblay, SER, "Vermont Yankee Nuclear Power Station, Safety Evaluation of FROSSTEY-2 Computer Code (TAC No. M68216)," NVY 92-178 (September 24, 1992).

10. Appendix A to Operating License DPR-28 Technical Specifications and Bases for Vermont Yankee Nuclear Power Station, Docket No. 50-271.

11. VYNPC Letter to USNRC, "Inverted Control Rod Poison Tubes at Vermont Yankee," WVY 75-51 (May 16, 1975).

12. USNRC Letter to G. C. Andognini, "Change to Bases," (June 6, 1975).

13. A. S. DiGiovine, et al.; CASMO-3 Validation; YAEC-1363-A (April 1988).

14. A. A. F. Ansari, Methods for the Analysis of Boiling Water Reactors: Steady-State Core Flow Distribution Code (FIBWR), YAEC-1234 (December 1980).

15. A. A. F. Ansari, R. R. Gay, and B. J. Gitnick; FIBWR: A Steady-State Core Flow Distribution Code for Boiling Water Reactors - Code Verification and Qualification Report; EPRI NP-1923; Project 1754-1 Final Report (July 1981).

16. USNRC Letter to J. B. Sinclair, SER, "Acceptance for Referencing in Licensing Actions for the Vermont Yankee Plant of Reports: YAEC-1232, YAEC-1238, YAEC-1299P, and YAEC-1234," NVY 82-157 (September 15, 1982).

17. GE Letter, J. L. Tuttle to R. T. Yee, "SLMCPR Calculation for Vermont Yankee Reload 18/Cycle 19," JLT96035 (August 5, 1996).

18. USNRC Letter to D. A. Reid, "Issuance of Amendment for Vermont Yankee Nuclear Power Station (TAC No. M96304)," NVY96-154 (October 4, 1996).

19. General Electric Company, GEXL-Plus Correlation Application to BWR 2-6 Reactors GE6 through GE9 Fuel, NEDE-31598P, GE Company Proprietary (July 1989).

20. GE Letter, J. L. Tuttle to R. T. Yee, "Revised Thermal-Mechanical MAPLHGR Limits for Vermont Yankee Reload 18/Cycle 19," JLT96044 (August 14, 1996).

21. GE Letter, D. T. Weiss to R. T. Yee, "Fuel Rod Thermal-Mechanical Performance Limits," DTW92260 (November 19, 1992).

22. A. A. F. Ansari and J. T. Cronin, Methods for the Analysis of Boiling Water Reactors: A Systems Transient Analysis Model (RETRAN), YAEC-1233, (April 1981).

23. USNRC Letter to R. L. Smith, SER, "Amendment No. 70 to Facility License No. DPR-28," (November 27, 1981).

24. V. Chandola, M. P. LeFrancois, and J. D. Robichaud; Application of One-Dimensional Kinetics to Boiling Water Reactor Transient Analysis Methods; YAEC-1693-A, Revision 1 (November 1989).

25. Electric Power Research Institute, RETRAN - A Program for One-Dimensional Transient Thermal-Hydraulic Analysis of Complex Fluid Flow Systems, CCM-5 (December 1978).

26. USNRC Letter to T. W. Schnatz, SER, "Acceptance for Referencing of Licensing Topical Reports: EPRI CCM-5 and EPRI NP-1850-CCM," (September 4, 1984).

27. A. A. F. Ansari, K. J. Burns, and D. K. Beller; Methods for the Analysis of Boiling Water Reactors: Transient Critical Power Ratio Analysis (RETRAN-TCPYA01); YAEC-1299P (March 1982).

28. J. T. Cronin, Method for Generation of One-Dimensional Kinetics Data for RETRAN-02, YAEC-1694-A (June 1989).

29. General Electric Company; C. J. Paone, et al.; Rod Drop Accident Analysis for Large Boiling Water Reactors; NEDO-10527 (March 1972).

30. General Electric Company; R. C. Stirn, et al.; Rod Drop Accident Analysis for Large Boiling Water Reactors Addendum No. 1, Multiple Enrichment Cores with Axial Gadolinium; NEDO-10527, Supplement 1 (July 1972).

31. General Electric Company; R. C. Stirn, et al.; Rod Drop Accident Analysis for Large Boiling Water Reactor Addendum No. 2 Exposed Cores; NEDO-10527, Supplement 2 (January 1973).

32. General Electric Company, C. J. Paine, Banked Position Withdrawal Sequence, NEDO-21231 (January 1977).

33. General Electric Company, D. Radcliffe and R. E. Bates, Reduced Notch Worth Procedure, SIL-316 (November 1979).

34. M. A. Sironen, Vermont Yankee Cycle 14 Core Performance Analysis Report, YAEC-1706 (October 1988).

35. USNRC Letter to L. A. Tremblay, SER, "Safety Evaluation for Vermont Yankee Nuclear Power Station RELAP5YA LOCA Analysis Methodology (TAC No. M74595)," NVY 92-192 (October 21, 1992).

36. USNRC Letter to R. W. Capstick, SER, "Approval of Use of Thermal-Hydraulic Code RELAP5YA (TAC No. 60193)," NVY 87-136 (August 25, 1987).

37. L. Schor, et al.; Vermont Yankee Loss-of-Coolant Accident Analysis; YAEC-1772 (June 1993).

38. Report, RELAP5YA, A Computer Program for Light-Water Reactor System Thermal-Hydraulic Analysis, YAEC-1300P-A, Revision 0, October 1982; Revision 1 (July 1993).

39. M. A. Sironen, Vermont Yankee Cycle 18 Core Performance Analysis Report, YAEC-1908, Rev. 1 (November 1995).

40. Vermont Yankee Nuclear Power Station Final Safety Analysis Report, Rev. 13, 1995.

41. Report, General Electric Nuclear Energy, BWR Owners' Group Long-Term Solutions Licensing Methodology, NEDO-31960-A and Supplement 1 (November 1995).

42. N. Fujita, M. P. LeFrancois and R. J. Weader, Method for Power/Flow Exclusion Region Calculation Using the LAPUR5 Computer Code, YAEC-1926 (September 1995).

43. Report, General Electric Nuclear Energy, BWR Owners' Group Reactor Stability Detect and Suppress Solutions Licensing Basis Methodology and Reload Applications, NEDO-32465 (May 1995).

44. Report, General Electric Nuclear Energy, Application of the "Regional Exclusion with Flow Biased Scram APRM Neutron Flux Scram" Stability Solution (Option 1-D) to the Vermont Yankee Nuclear Power Plant, GENE-637-018-0793 (July 1993).

45. VYNPC Letter to USNRC, "Cycle 18 Startup Test Report," BVY 95-81 (July 25, 1995).

APPENDIX A

CALCULATED OPERATING LIMITS

The MCPR operating limits for the Reload Cycle are calculated by adding the calculated ΔCPR to the FCISL. This is done for each of the analyses in Section 7.0 at each of the exposure statepoints. For an exposure interval between statepoints, the highest MCPR limit at either end is assumed to apply to the whole interval.

Table A.1 provides the highest calculated MCPR limits for the Reload Cycle for each of the exposure intervals for the various scram speeds and for the various rod block lines. These MCPR operating limits are valid for operation of the Reload Cycle at full power up to 10701 MWd/St and for operation during coastdown beyond EOFPL.

Tables A.2 through A.4 provide the most limiting calculated MAPLHGR limits for all the fuel types in the Reload Cycle. These values bound the lattice-specific MAPLHGR limits for all the enriched lattice zones in each fuel type. The MAPLHGR limits were revised for the LOSC transient results.

Table A.5 provides the actual power and flow values used in the generation of the stability exclusion and buffer regions. Figure A.1 provides the stability exclusion and buffer region curves.

TABLE A.1

VERMONT YANKEE NUCLEAR POWER STATION
CYCLE 19 MCPR OPERATING LIMITS

Value of "N" in RBM Equation[1]	Average Control Rod Scram Time	Cycle Exposure Range	MCPR Operating Limit[2,3]
42%	Equal to or better than L.C.O. 3.3.C.1.1	0.0 to 9701 MWd/St	1.32
		9701 to 10701 MWd/St	1.34
	Equal to or better than L.C.O. 3.3.C.1.2	0.0 to 9701 MWd/St	1.32
		9701 to 10701 MWd/St	1.41
41%	Equal to or better than L.C.O. 3.3.C.1.1	0.0 to 9701 MWd/St	1.29
		9701 to 10701 MWd/St	1.34
	Equal to or better than L.C.O. 3.3.C.1.2	0.0 to 8701 MWd/St	1.29
		8701 to 9701 MWd/St	1.32
		9701 to 10701 MWd/St	1.41
≤ 40%	Equal to or better than L.C.O. 3.3.C.1.1	0.0 to 9701 MWd/St	1.29
		9701 to 10701 MWd/St	1.34
	Equal to or better than L.C.O. 3.3.C.1.2	0.0 to 8701 MWd/St	1.29
		8701 to 9701 MWd/St	1.32
		9701 to 10701 MWd/St	1.41

(1) The Rod Block Monitor (RBM) trip setpoints are determined by the equation shown in Table 3.2.5 of the Technical Specifications.

(2) The current analysis for the MCPR operating limits does not include the 7X7, 8X8, 8X8R or P8X8R fuel types. On this basis, if any of these fuel types are to be reinserted, they will be evaluated in accordance with 10CFR50.59 to ensure that the above limits are bounding for these fuel types.

(3) MCPR operating limits should be increased by 0.02 for the single loop operation.

TABLE A.2

MAPLHGR VERSUS AVERAGE PLANAR EXPOSURE FOR BP8DWB335-10GZ

Plant: Vermont Yankee

Fuel Type: BP8DWB335-10GZ

Average Planar Exposure	MAPLHGR Limits (kW/ft)	
(MWd/St)	Two-Loop Operation	Single-Loop Operation*
0.00	11.29	9.37
200.00	11.34	9.41
1,000.00	11.48	9.53
2,000.00	11.69	9.70
3,000.00	11.92	9.89
4,000.00	12.17	10.10
5,000.00	12.43	10.32
6,000.00	12.68	10.52
7,000.00	12.87	10.68
8,000.00	13.06	10.84
9,000.00	13.20	10.96
10,000.00	12.79	10.62
12,500.00	12.65	10.50
15,000.00	12.47	10.35
20,000.00	11.76	9.76
25,000.00	11.09	9.20
35,000.00	9.88	8.20
45,000.00	8.38	6.96
50,590.00	5.65	4.69

* MAPLHGR limits for single-loop operation are obtained by multiplying the two-loop operation MAPLHGR limits by 0.83.

TABLE A.3

MAPLHGR VERSUS AVERAGE PLANAR EXPOSURE FOR BP8DWB335-11GZ

Plant: Vermont Yankee

Fuel Type: BP8DWB335-11GZ

Average Planar Exposure	MAPLHGR Limits (kW/ft)	
(MWd/St)	Two-Loop Operation	Single-Loop Operation*
0.00	11.28	9.36
200.00	11.33	9.40
1,000.00	11.43	9.49
2,000.00	11.60	9.63
3,000.00	11.80	9.80
4,000.00	12.04	9.99
5,000.00	12.30	10.21
6,000.00	12.53	10.40
7,000.00	12.73	10.57
8,000.00	12.94	10.74
9,000.00	13.12	10.89
10,000.00	12.79	10.62
12,500.00	12.65	10.50
15,000.00	12.47	10.35
20,000.00	11.76	9.76
25,000.00	11.09	9.20
35,000.00	9.88	8.20
45,000.00	8.38	6.96
50,590.00	5.65	4.69

* MAPLHGR limits for single-loop operation are obtained by multiplying the two-loop operation MAPLHGR limits by 0.83.

TABLE A.4

MAPLHGR VERSUS AVERAGE PLANAR EXPOSURE FOR BP8DWB354-12GZ

Plant: Vermont Yankee

Fuel Type: BP8DWB354-12GZ

Average Planar Exposure	MAPLHGR Limits (kW/ft)	
(MWd/St)	Two-Loop Operation	Single-Loop Operation*
0.00	10.96	9.10
200.00	11.04	9.16
1,000.00	11.18	9.28
2,000.00	11.40	9.46
3,000.00	11.63	9.65
4,000.00	11.81	9.80
5,000.00	12.01	9.97
6,000.00	12.14	10.08
7,000.00	12.26	10.18
8,000.00	12.37	10.27
9,000.00	12.46	10.34
10,000.00	12.52	10.39
12,500.00	12.40	10.29
15,000.00	12.10	10.04
20,000.00	11.40	9.46
25,000.00	10.72	8.90
35,000.00	9.44	7.84
45,000.00	7.24	6.01
48,200.00	5.67	4.71

* MAPLHGR limits for single-loop operation are obtained by multiplying the two-loop operation MAPLHGR limits by 0.83.

TABLE A.5

VERMONT YANKEE NUCLEAR POWER STATION

CYCLE 19 STABILITY EXCLUSION AND BUFFER REGIONS

Exclusion Region		Buffer Region	
Flow	Power	Flow	Power
27.000	34.2602	27.8420	29.4008
28.000	34.5125	29.5823	29.8049
29.000	34.9275	31.2232	30.4723
30.000	35.5053	32.7519	31.3477
31.000	36.2458	34.1750	32.3963
32.000	37.1492	35.5083	33.5970
33.000	38.2154	36.7696	34.9390
34.000	39.4443	37.9747	36.4180
35.000	40.8360	39.1369	38.0338
36.000	42.3905	40.2661	39.7879
37.480	44.9900	41.8927	42.6430
38.000	45.9879	42.4546	43.7209
39.000	48.0308	43.5238	45.9047
40.000	50.2364	44.5812	48.2365
41.000	52.6049	45.6292	50.7181
41.970	55.0578	46.6385	53.2701
43.000	57.8301	47.7040	56.1376
44.000	60.6869	48.7334	59.0781
45.000	63.7065	49.7587	62.1739
46.000	66.8889	50.7806	65.4260
47.000	70.2340	51.7998	68.8350
48.000	73.7420	52.8166	72.4017
49.700	80.0791	54.5407	78.8284
50.000	81.2461	54.8445	80.0102
51.000	85.2425	55.8561	84.0529
51.660	88.0000	56.8665	88.2552
		57.7330	92.0000
		57.8758	92.6173

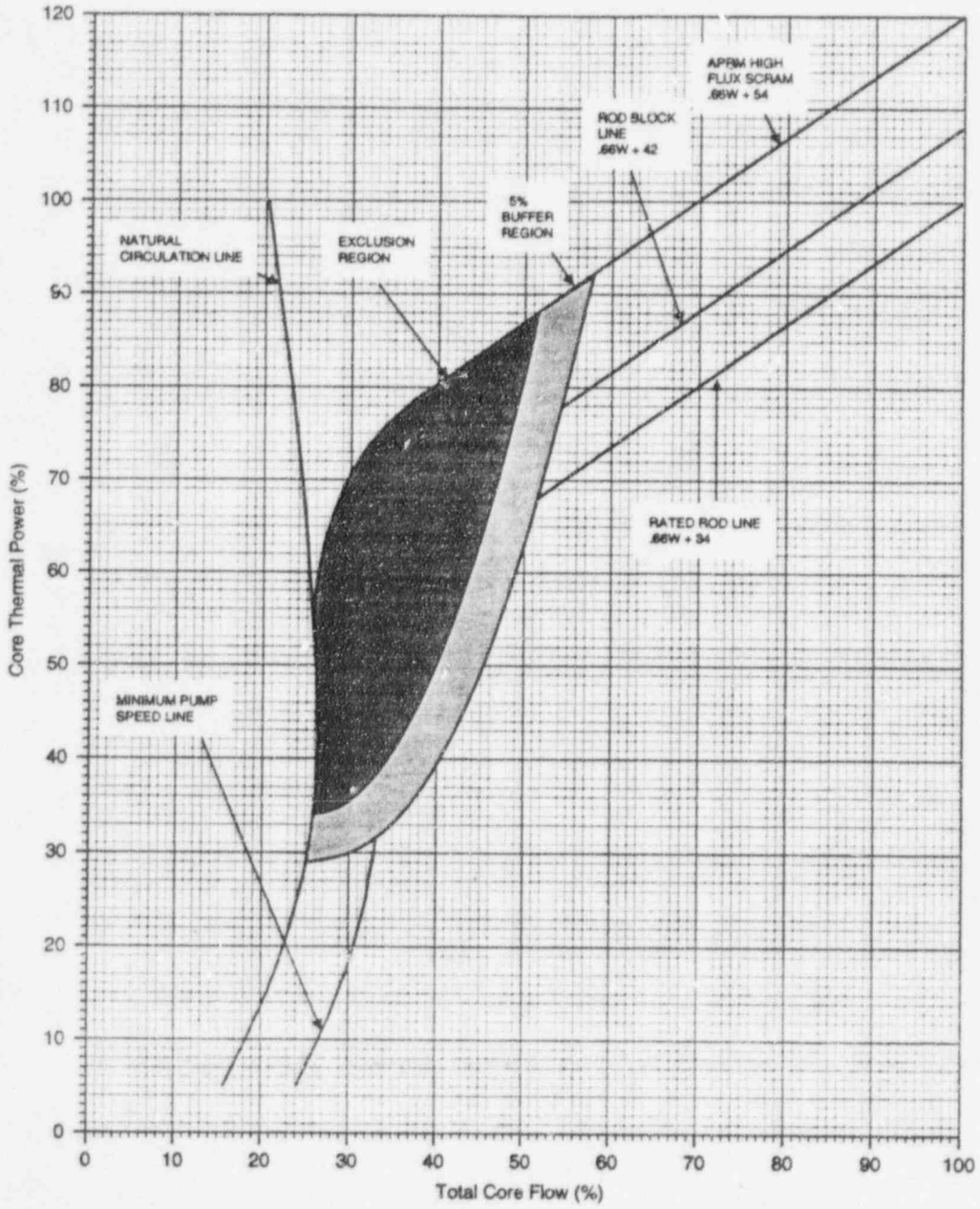

FIGURE A.1

VERMONT YANKEE NUCLEAR POWER STATION

CYCLE 19 STABILITY EXCLUSION AND BUFFER REGIONS